CONTACT INFORMATION
Mining Records Curator
Arizona Geological Survey
3550 N. Central Ave, 2nd floor
Phoenix, AZ, 85012
602-771-1601
http://www.azgs.az.gov
inquiries@azgs.az.gov

The following file is part of the Cambior Exploration USA Inc. records

ACCESS STATEMENT

These digitized collections are accessible for purposes of education and research. We have indicated what we know about copyright and rights of privacy, publicity, or trademark. Due to the nature of archival collections, we are not always able to identify this information. We are eager to hear from any rights owners, so that we may obtain accurate information. Upon request, we will remove material from public view while we address a rights issue.

CONSTRAINTS STATEMENT

The Arizona Geological Survey does not claim to control all rights for all materials in its collection. These rights include, but are not limited to: copyright, privacy rights, and cultural protection rights. The User hereby assumes all responsibility for obtaining any rights to use the material in excess of "fair use."

The Survey makes no intellectual property claims to the products created by individual authors in the manuscript collections, except when the author deeded those rights to the Survey or when those authors were employed by the State of Arizona and created intellectual products as a function of their official duties. The Survey does maintain property rights to the physical and digital representations of the works.

QUALITY STATEMENT

The Arizona Geological Survey is not responsible for the accuracy of the records, information, or opinions that may be contained in the files. The Survey collects, catalogs, and archives data on mineral properties regardless of its views of the veracity or accuracy of those data.

Economic Geology
Vol. 85, 1990, pp. 29–49

Stratigraphy and Alteration of the Host Rocks, United Verde Massive Sulfide Deposit, Jerome, Arizona

MAE SEXAUER GUSTIN*

Department of Geosciences, The University of Arizona, Tucson, Arizona 85721

Abstract

The early Proterozoic volcanogenic United Verde massive sulfide orebody is situated within the Cleopatra Member of the Deception Rhyolite. The Cleopatra Member, a porphyritic rhyodacite, has been subdivided into an upper unit and a lower unit. The United Verde orebody, previously interpreted to lie at the top of the Cleopatra Member, is now recognized as lying within the basal section of the upper unit of the Cleopatra Member.

The upper unit and lower unit are differentiated on the basis of alteration mineralogy, mineral and rock geochemistry, and lithologic peculiarities. The contact between the two units is marked by sediments at the base of the upper unit, including a distinct green calcite-bearing feldspar tuff, chert and hematitic chert layers, and a quartz porphyry conglomerate.

The Cleopatra Member contains six distinct alteration types. Five alteration types characterize the lower unit and include two types of moderate chloritic and sericitic alteration (designated B1 and B2), two spatially distinct types of sericitic and silicic alteration (designated S1 and S2), and an area of intense chloritic alteration (designated C). These five alteration types record the effects of hydrothermal alteration by the massive sulfide ore-forming system and of a regional greenschist facies metamorphic event. The upper unit contains the least altered rocks of the Cleopatra Member and the bulk of the sixth alteration type, designated H. The rocks included within H-type alteration have disseminated hematite and/or hematitic chert veining.

Whole-rock and mineral geochemistry of the lower unit may be used to establish position within the paleohydrothermal system. The distal area of moderate alteration (B1) contains samples enriched in MgO, slightly depleted in alkalies, and having ratios of $Fe_2O_{3(total)}/Fe_2O_{3(total)} + MgO$ for whole rocks and $Fe_{(total)}/Fe_{(total)} + Mg$ for chlorites that are low relative to other Cleopatra Member samples. These attributes are suggestive of the low-temperature seawater-rock interaction expected in the domain of fluid recharge. Rocks of alteration type C experienced significant additions of iron and magnesium, and losses of CaO, Na_2O, and K_2O, presumed to reflect alteration in the main discharge conduit for the hydrothermal fluid. Chlorite and whole-rock iron to iron-plus-magnesium ratios decrease within the area of alteration type C toward the sediment-water interface. This is consistent with mixing of an evolved ore-forming fluid with seawater in the upper levels of the area of alteration type C. Samples from the area of alteration type B2, which is intermediate between the recharge (B1) and discharge areas (C), are greatly depleted in CaO and Na_2O, and are enriched in iron. Alteration types S1 and S2 are interpreted to reflect localized sites of fluid discharge where SiO_2 and K_2O have been added and other major elements, except for Al_2O_3, have been removed.

Whole-rock and mineral chemistry of the alteration types record progressive changes in the hydrothermal fluid from seawater to an ore-forming fluid. The fluid that was discharging and depositing ore apparently had a log a_{O_2} between −41.7 and −35.5, a log a_{H_2S} between −5 and −2.6, and was saturated with respect to iron sulfides, magnesium silicates, and ore-forming metals.

Introduction

VOLCANIC-hosted syngenetic massive sulfide deposits are interpreted to have formed in association with convecting cells of heated seawater (cf. Spooner, 1977; Franklin et al., 1981; Pisutha-Arnond and Ohmoto, 1983; Muehlenbachs, 1986; Solomon et al., 1987). Variations in host-rock mineralogy, mineral chemistry, and rock geochemistry have been used to define recharge and discharge areas for the hydrothermal fluid associated with some massive sulfide forming systems (cf. MacGeehan, 1978; Franklin et al., 1981; Gregory and Taylor, 1981; Pisutha-Arnond and Ohmoto, 1983). For many massive sulfide deposits, especially those in Paleozoic and Precambrian terranes, the distribution of recharge and discharge

* Present address: 5187 Aspenview Drive, Reno, Nevada 89523.

0361-0128/90/1030/29-21$3.00

areas and the effects of hydrothermal alteration have been obscured by deformation and metamorphism.

The United Verde orebody is a stratiform volcanogenic massive sulfide deposit (Anderson and Nash, 1972; Lindberg and Jacobson, 1974; Anderson and Guilbert, 1979) that was formed on the sea floor at approximately 1.8 Ga (Anderson et al., 1971; Karlstrom et al., 1987). The orebody is located within the Cleopatra Member of the Deception Rhyolite, a unit composed of rhyodacitic lavas and volcaniclastic rocks. Distinct alteration types are recognized within the Cleopatra Member despite the superposition of regional deformation and metamorphism upon the hydrothermally altered rocks. Alteration types are used as one criterion for differentiation between the upper and lower units of the Cleopatra Member, and their distribution is indicative of recharge and discharge areas for a portion of the United Verde hydrothermal cell.

This paper presents the results of detailed mapping of alteration types within the Cleopatra Member, petrographic study of samples of the Cleopatra Member, and evaluation of whole-rock and mineral geochemical data from samples of the Cleopatra Member. Stable isotope data, also obtained during this research project, will be presented in another paper. The major contributions of the research presented in this paper are a breakdown of the Cleopatra Member into two units, a relocation of the stratigraphic position of the United Verde deposit, a description of the effects of the United Verde ore-forming hydrothermal cell on the Cleopatra Member, and an evaluation of the physicochemical nature of the hydrothermal system.

General Geology

The United Verde orebody is located in central Arizona in the transition zone between the Basin and Range and the Colorado plateau tectonic provinces. The orebody is the largest of the Proterozoic volcanogenic sulfide deposits exposed in this belt of rocks (Lindberg, 1986b). Approximately 30 million metric tons of 4.80 percent Cu, 1.61 oz/metric ton Ag, and 0.043 oz/metric ton Au, plus a small amount of zinc

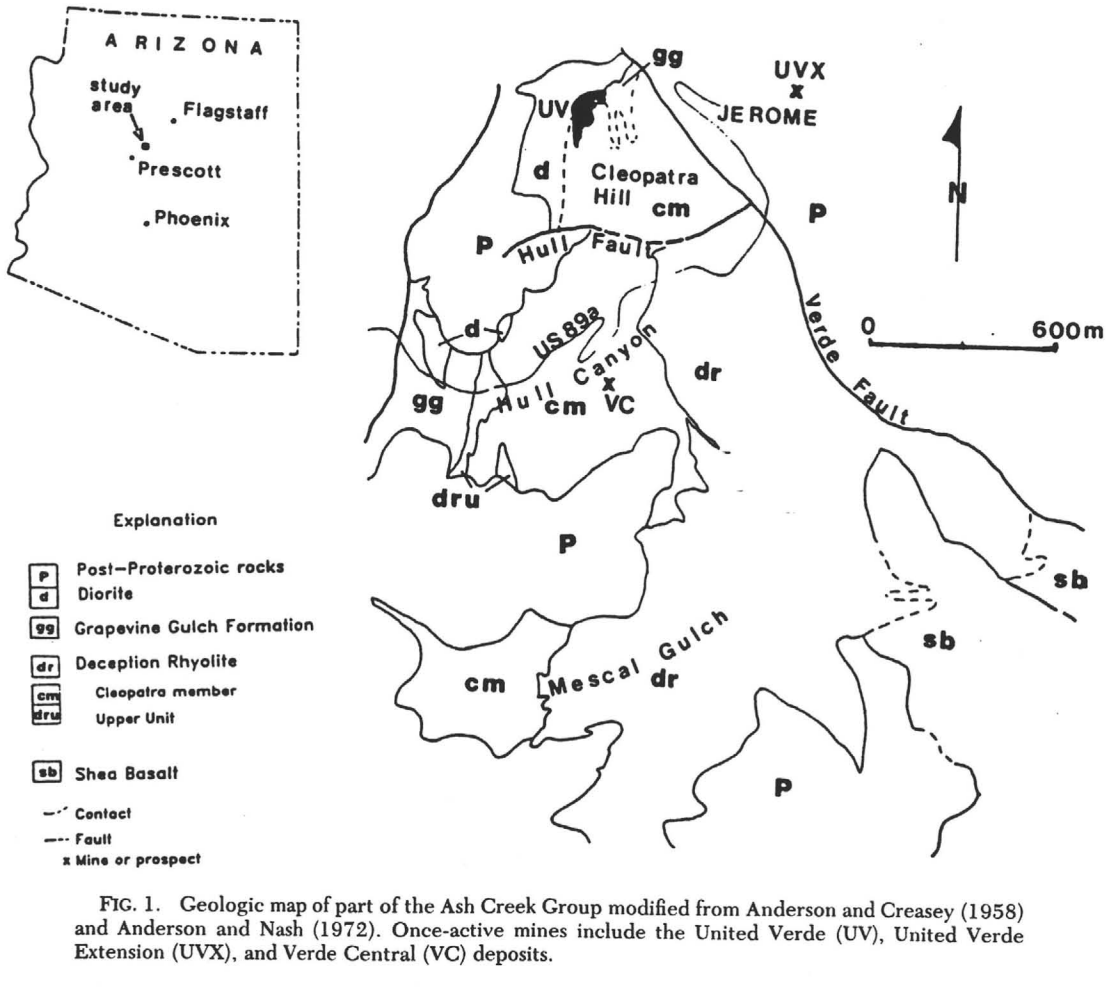

FIG. 1. Geologic map of part of the Ash Creek Group modified from Anderson and Creasey (1958) and Anderson and Nash (1972). Once-active mines include the United Verde (UV), United Verde Extension (UVX), and Verde Central (VC) deposits.

by-product, were produced from the United Verde deposit between 1883 and 1975 (Lindberg, 1988).

The United Verde orebody is included within the Deception Rhyolite of the Ash Creek Group of the Yavapai Series (Anderson et al., 1971). The Deception Rhyolite, which lies stratigraphically above the Shea Basalt (Fig. 1), was initially subdivided by Anderson and Creasey (1958) into an upper unit and lower unit. The Cleopatra Member was considered by them to represent an intrusive body that postdated the Deception Rhyolite. Anderson and Nash (1972) recognized that the Cleopatra contained extrusive units and included it as a member within the Deception Rhyolite. In this paper the Cleopatra is retained as a member of the Deception Rhyolite. The upper and lower units of the Deception Rhyolite (Anderson and Creasey, 1958), located stratigraphically below the Cleopatra Member, are lumped as the Deception Rhyolite (Fig. 1). Based on lithologic similarity to the Cleopatra Member, a small lens of the upper unit of the Deception Rhyolite of Anderson and Creasey (1958) and Anderson and Nash (1972), located south of highway 89a, is now recognized as a component of the upper unit of the Cleopatra Member (cf. Figs. 1 and 2). The largest area of outcrop of Anderson and Creasey's (1958) upper unit (upper succession rhyolite; Lindberg, 1986a) is traversed by U. S. 89a (Fig. 1) and is a fine-grained dacitic unit with sediments marking its base. It is locally silicified and hematitized and is distinctively different from the Cleopatra Member. This small localized unit is herein included within the Grapevine Gulch Formation for simplicity. The Grapevine Gulch Formation consists of turbidite sediments intercalated with andesitic and dacitic volcanic rocks. It overlies the Cleopatra Member.

A metadioritic intrusion has concealed the hanging wall above the massive sulfide body and, in general, is concordant to bedding (Anderson and Creasey, 1958; Lindberg, 1986a) (Fig. 1). The Proterozoic rocks of the Ash Creek Group are overlain unconformably by Paleozoic sediments.

Metamorphism of the Ash Creek Group has not been definitively constrained. Lanphere (1968) obtained Rb-Sr whole-rock ages for metamorphism of 1,640 to 1,660 Ma. However, the Cherry Creek batholith, which is 7 km to the south of the United Verde mine, is postfolding (Anderson and Creasey, 1958) and has been dated at 1,740 ± 15 Ma (Anderson et al., 1971; Karlstrom et al., 1987). Formations within the study area, the upper Shea Basalt, the Deception Rhyolite, and the Grapevine Gulch Formation, are characterized by the mineral assemblage sericite + chlorite + quartz + albite, indicative of lower greenschist facies metamorphism (Turner and Verhoogen, 1960; Winkler, 1979). Vance and Condie (1987) reported an assemblage of sericite + chlorite + oligoclase for the felsic rocks of the study area and

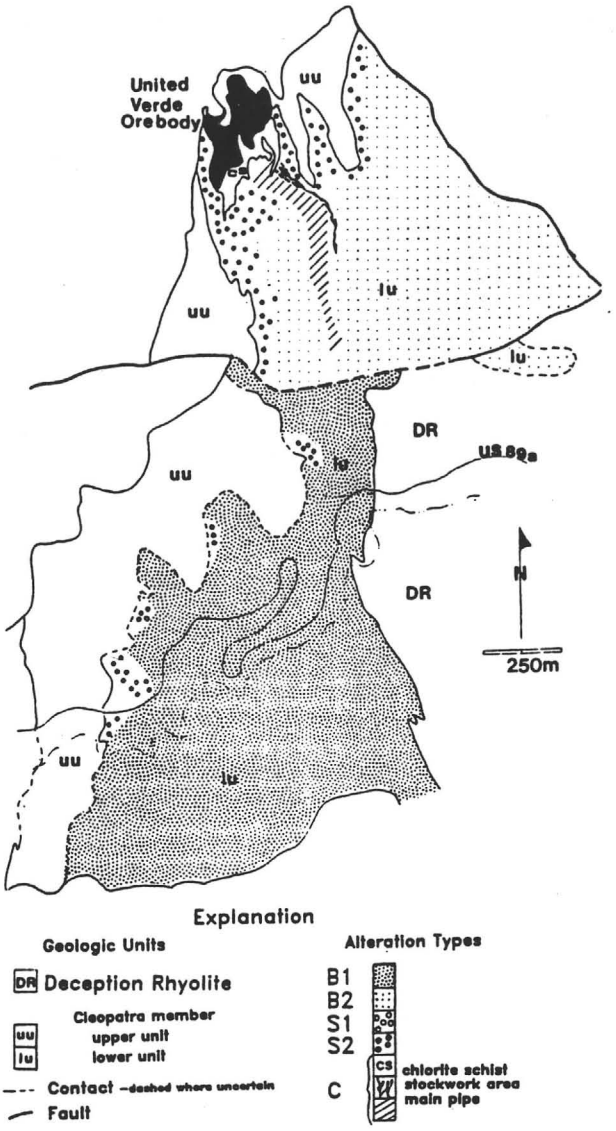

FIG. 2. Geologic map of the Cleopatra Member showing exposures of alteration types of the lower unit. Upper and lower Cleopatra Member boundaries are adapted from Anderson and Creasey (1958). See Table 2 for description of alteration types.

suggested metamorphic conditions transitional between greenschist and amphibolite facies. Microprobe analyses of samples from the Cleopatra Member (Table 1) indicate that the feldspar is albite, suggesting that metamorphic conditions were not as high as Vance and Condie (1987) predicted for the study area. However, it is possible that higher grade metamorphic facies occur to the south of the study area in the Copper Chief mine area, where hornblende has been reported (Vance and Condie, 1987; D. Armstrong, pers. commun., 1988).

A minimum of two episodes of deformation were superimposed upon the Ash Creek Group (Anderson

TABLE 1. Electron Microprobe Analyses and Structural Formulas of Feldspar from the Cleopatra Member

	Lower unit		Upper unit		
Sample no.	157	75	127	205	117
Number of analyses	3	3	2	4	4
	Wt percent oxides				
Na_2O	11.27	12.10	11.19	11.47	10.36
K_2O	0.21	0.11	0.19	0.06	1.35
CaO	0.18	0.18	1.09	0.86	0.86
Al_2O_3	19.64	19.51	20.19	19.90	20.49
SiO_2	67.49	68.50	66.00	66.33	67.82
Total	98.79	100.40	98.66	98.62	100.88
	Molecules per 32 oxygens				
Na	3.83	4.09	3.82	3.95	3.51
K	0.05	0.02	0.042	0.013	0.25
Ca	0.03	0.03	0.205	0.16	0.16
Al	4.06	4.01	4.19	4.17	4.22
Si	11.96	11.94	11.78	11.79	11.86

and Creasey, 1958; Lindberg 1986a). All rocks have been penetratively deformed into near-isoclinal folds (Lindberg, 1986a; Lindberg and Gustin, 1987).

Cleopatra Member

Lithologic units

The Cleopatra Member has been subdivided into two units, designated as the upper and lower units. Both these units consist predominantly of porphyritic rhyodacitic lavas and volcaniclastic rocks. One- to four-mm-wide quartz and plagioclase phenocrysts may make up 10 to 40 percent of a hand sample. These phenocrysts characterize the Cleopatra Member and render it a distinct lithostratigraphic unit.

The Cleopatra Member was originally considered to be a felsic intrusion (Anderson and Creasey, 1958). Kothavala (1963), however, recognized that the member contained a high percentage of extrusive rocks; Anderson and Nash (1972) subsequently reinterpreted the unit as a package of intertonguing flow-banded porphyritic rock, breccia, and tuff. Lindberg (1986a) called the unit the Cleopatra crystal tuff and Anderson (1986) described the unit as consisting of phenocrystic agglomerate and quartz crystal ash-flow tuff.

Mapping for this study indicated that the Cleopatra Member comprises lava flows and shallow intrusions, vitroclastic tuffs, and fine- to coarse-grained volcaniclastic rocks. Lava flows are most abundant in the lower unit on Cleopatra Hill, which is located between the Hull fault and the orebody, and in Mescal Gulch (Fig. 1). Medium- to coarse-grained volcaniclastic rocks abound between these two areas.

The upper unit contains a higher percentage of clastic rocks than the lower unit. Coarse-grained volcaniclastic rocks and some lava flows or high-level intrusions occur at the stratigraphic base and intermediate levels. Fine- to coarse-grained sediments and crystal tuffs are abundant at the stratigraphic top.

The United Verde massive sulfide deposit and an eastward-thickening package of epiclastic and chemical sediments occur at the base of the newly defined upper unit. Sediments and chemical precipitates include chert, hematitic chert, fine- to medium-grained volcaniclastic sediments, a dolomite-chlorite lens, and conglomeratic layers. A green calcite-bearing feldspar crystal tuff is a marker unit for the base of the upper unit south of the orebody. A comparable green tuff from the hanging wall to the orebody in underground exposures is described (Hansen, 1930; Kothavala, 1963; Anderson and Nash, 1972).

Several outcrops of sediments exposed in the walls and floor of the United Verde open-pit area, previously interpreted to represent the Grapevine Gulch Formation (Fig. 1; Anderson and Creasey, 1958; Anderson and Nash, 1972; Lindberg, 1986a), are now interpreted as the basal portion of the upper unit (Gustin, 1988; Fig. 2). These sediments are interpreted to have been deposited at approximately the same time as the United Verde orebody, based on their stratigraphic position and the presence of sulfide-rich interlayers in the sediments. Lindberg (1986a) notes that the chert layers in the sediments exposed in the southwest wall of the pit are coeval with the United Verde orebody, also suggesting that the sediments with which they are interbedded are coeval with the orebody.

Most of the upper unit in the immediate hanging wall to the United Verde orebody is concealed by a postore metadiorite intrusion. Units that are exposed and described as occurring in underground exposures include the green calcite-bearing feldspar tuff, hematite-bearing tuffaceous units, and cherts (Hansen, 1930; Kothavala, 1963; Anderson and Nash, 1972). A quartz-feldspar porphyry with lithologic characteristics and chlorite chemistry similar to the upper unit overlies the United Verde Extension orebody (P. A. Handverger, oral commun., 1975). Lindberg (1986a) has proposed that the United Verde Extension orebody formed contemporaneously with the United Verde orebody. The presence of a hanging-wall rock similar to the upper unit overlying the United Verde Extension orebody suggests that the upper unit may have overlain the United Verde but was largely concealed by the intrusion.

On the basis of the distribution of lithologic types in the lower unit of the Cleopatra Member, it is possible that massive flows accumulated or domes formed in the vicinity of the United Verde orebody and in Mescal Gulch. Deposition of medium- to coarse-grained volcaniclastic rocks between these two areas

was perhaps a result of slumping of material off the two areas of massive lavas. The United Verde orebody was deposited during a period of volcanic quiescence on the edge of a basin. This is suggested by the fact that the sediments that crop out to the east and west of the orebody in the basal upper unit thicken to the east. Following deposition of the basal sediments of the upper unit, renewed volcanic activity introduced predominantly volcaniclastic rocks with minor massive flows. Diminished volcanic activity is recorded at the top of the upper unit by the preponderance of clastic sediments and chert layers.

Lindberg (1986a) proposed that the United Verde ore-forming fluids were ponded against a fault exposed on the southwest face of the United Verde open pit. He suggested that this fault was a product of caldera collapse responsible for extrusion of the Cleopatra Member. The contact exposed in the southwest wall of the open pit is that between the upper unit and lower unit; there is no evidence of a fault scarp. There is no geologic evidence to suggest that caldera collapse was responsible for extrusion of the Cleopatra Member. There is no apparent ring fracture system. There are also no abundant broken crystals, evidence of abundant glass and pumice, welded textures, or signs of graded bedding, all reported by Fiske and Matsuda (1964) as common components of subaqueous pyroclastic flow deposits. This is not to say Lindberg's model is incorrect but that there is little geologic evidence to support such a model.

Petrography

Phenocrysts in least altered lower unit samples (alteration type B1, Fig. 2) include quartz, some with well-developed secondary overgrowths and resorption textures, and sericitized albite. In more altered samples, albite has been completely removed or replaced by polycrystalline quartz pseudomorphs. The groundmass is characterized by 20 to 30 percent, 0.1- to 0.2-mm, subrounded to subangular polycrystalline quartz aggregates surrounded by a matrix of finer grained recrystallized quartz, sericite, and chlorite. Trace amounts of zircon, rutile, and calcite are also present.

The polycrystalline quartz aggregates have been described by previous writers as clasts in a tuffaceous unit (Anderson and Nash, 1972) and as products of intense granulation due to shearing during folding (Vance and Condie, 1987). I suggest that the aggregates were products of hydrothermal alteration and subsequent metamorphism and deformation. During hydrothermal alteration both quartz and the phyllosilicate minerals were added to the rock. Following alteration, metamorphism and deformation are interpreted to have caused the quartz and phyllosilicates to segregate into discrete domains. The polycrystalline nature of the quartz aggregates suggests that their present texture is metamorphic in origin.

The polycrystalline quartz aggregates are found in outcrops of lava flows, vitroclastic lapilli tuffs, and volcaniclastic rocks that contain at least 20 percent chlorite and/or sericite. Kothovala (1963) describes similar textures in chloritized samples of the upper Shea Basalt. The upper unit and some distal (>1 km from the United Verde orebody) lower unit outcrops do not exhibit this texture. This is presumably because they did not contain the requisite amount of phyllosilicate minerals necessary for segregation of the minerals into distinct domains.

Samples of the upper unit, in contrast to the lower unit, typically exhibit a groundmass that is an aphanitic equigranular mixture of quartz, feldspar, and sericite. In general, quartz phenocrysts of the upper unit do not exhibit secondary overgrowths. Albite phenocrysts are slightly calcic in composition (Table 1), and mildly saussuritized and sericitized.

Alteration

The lower unit of the Cleopatra Member contains essentially no unaltered rocks. Rocks of the lower unit exhibit widespread alteration which is identified by the addition of moderate amounts of chlorite and sericite. Two types of moderate chloritic and sericitic alteration are present, designated B1 and B2 (Table 2). Also present are localized areas of sericitic and silicic alteration (designated S1 and S2) and an area where chlorite metasomatism was the dominant hydrothermal process (designated alteration type C). The upper unit contains the least-altered volcanic rocks of the Cleopatra Member. However, much of the upper unit has been affected by hematitic and silicic alteration, designated as alteration type H.

Vance and Condie (1987) studied alteration immediately beneath the orebody on Cleopatra Hill. They defined three zones of alteration. Their zone 1 corresponds with the zone of chlorite schist of alteration type C; their zone 2 includes some of both the area of alteration type C and rocks subjected to B2-type alteration; and their zone 3 includes both B2-

TABLE 2. Alteration Types of the Cleopatra Member

Alteration type	Mineral assemblage
B1	Albite + quartz + sericite + chlorite + calcite
B2	Quartz + chlorite + sericite
S1	Quartz + sericite ± carbonate ± chlorite
S2	Quartz + sericite + carbonate + sulfides
C	Quartz + chlorite ± sulfides ± ankerite ± monazite ± leucoxene
H	Albite + quartz + hematite + sericite ± chlorite ± calcite ± epidote

type alteration of the lower unit and H-type alteration in the upper unit.

Areas of moderate alteration (B1 and B2) are characterized by the mineral assemblage chlorite + sericite + quartz ± albite ± calcite. This assemblage is the result of both hydrothermal alteration and metamorphism. During hydrothermal alteration, primary minerals and volcanic glass were most likely altered to phyllosilicate minerals and zeolites similar to unmetamorphosed kuroko deposits (Urabe et al., 1983). Superposition of the metamorphic event changed the mineral assemblage to one that was stable at greenschist facies conditions, but, as will be demonstrated, the chemical composition of rocks and mineral phases is distinctive for each of the two areas of moderate alteration.

The area of B1-type alteration comprises the least altered outcrops of the lower unit and, unlike B2-type alteration, contains calcite and albite. Volcaniclastic rocks are mildly chloritized and sericitized, whereas flows appear relatively unaltered. More extensive alteration of the volcaniclastic rocks suggests that they were permeable to fluid flow.

In the area of B2-type alteration, feldspars have been replaced by quartz, chlorite, and/or sericite. A few polycrystalline quartz pseudomorphs attest to the previous presence of feldspar phenocrysts. Replacement of feldspar phenocrysts by quartz is also typical of kuroko deposits in the sericite-chlorite zone that surrounds the feeders and orebodies (Green et al., 1983). Quartz overgrowths on quartz phenocrysts and feldspar pseudomorphs are irregularly corroded by chlorite and sericite.

The rock matrix of samples from the area of B2 alteration ranges from a mixture of sericite, chlorite, and quartz to one of only chlorite and quartz. In some samples, relict islands of fine-grained chlorite float in a sericite-quartz matrix and sericite veinlets crosscut areas of chloritization. These textures suggest that sericitization postdated chloritization.

Vance and Condie (1987) describe chlorite as corroding quartz phenocrysts prior to development of secondary quartz overgrowths in samples from B2- and C-type alteration. Textural evidence for this inference was not observed in this study. Instead, chlorite, concentrated on the contact between the quartz grain and the secondary overgrowth, is interconnected to the rock groundmass by veinlets crosscutting the overgrowth. This, along with the observation that quartz overgrowths are corroded by chlorite and sericite, suggests that selective hydrothermal alteration occurred along a zone of weakness in the quartz grain and that chlorite corrosion postdates overgrowth development and silicification.

Alteration types S1 and S2 consist of the mineral assemblage quartz + sericite ± carbonate ± chlorite ± sulfides. Areas of the S1 type crop out as semiconformable resistant lenses along the top of the lower unit. One area of S1 alteration exhibits a zoned distribution of silica concentration, with quartz content increasing toward the center of the area. The silicified center is interpreted to be a site of focused fluid discharge. S2-type alteration surrounds the chlorite pipe and, unlike S1, contains sulfide minerals and ankerite. The carbonate mineral in areas of S1-type alteration is dolomite north of the Hull fault and calcite south of the fault (Gustin, 1988).

The area of type-C alteration, referred to below as the chlorite pipe, is interpreted to be the principal hydrothermal fluid discharge area. It is characterized by the alteration mineral assemblage chlorite ± quartz ± sulfides ± ankerite ± monazite ± rutile ± leucoxene. The chlorite pipe is subdivided into three zones on the basis of mineralogy: the chlorite schist zone, the stockwork zone, and the main pipe (Fig. 2). The area immediately beneath the orebody, the chlorite schist zone, consists predominantly of chlorite, with lesser amounts of quartz and sulfides and minor leucoxene and monazite. The rock type that characterizes this area is best known as black schist (Anderson and Creasey, 1958; Anderson and Nash, 1972). The chlorite schist represents the lower unit completely replaced by two generations of chlorite. These two generations of chlorite were found to be chemically indistinguishable on the basis of microprobe analyses. The early generation of chlorite commonly consists of fine-grained low birefringence chlorite and is veined by the late coarse-grained generation of chlorite. The latter is characterized by anomalous interference colors. Islands of quartz are corroded by chlorite.

The chlorite schist zone has a gradational contact with the massive sulfide orebody (Anderson and Creasey, 1958) and with the main pipe and stockwork zones (Figs. 2 and 3). Samples from the main pipe are distinguished from the chlorite schist by the presence of contorted quartz-ankerite veins and the absence of sulfide minerals. Monazite, which occurs as elongate trains of anhedral crystals, is most abundant in this zone of C-type alteration. As exposed on Cleopatra Hill (Fig. 2) from north to south, the pipe grades from a completely chloritized lower unit to a recognizable lower unit with a pervasively chloritized matrix and minor quartz veining. As in the chlorite schist, the upper level of the main pipe contains two generations of chlorite. Angular clasts of fine-grained low birefringence chlorite and fragments of contorted quartz-ankerite veins are surrounded and crosscut by relatively coarse grained high birefringence chlorite. These textures suggest brecciation of the first-formed fine-grained chlorite and of the quartz-ankerite veins. This is interpreted to reflect hydrothermal processes

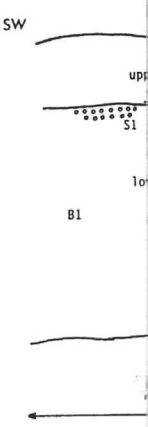

FIG. 3. Inte
constructed to
prior to deform
unit are denote
same as in Fig
types.

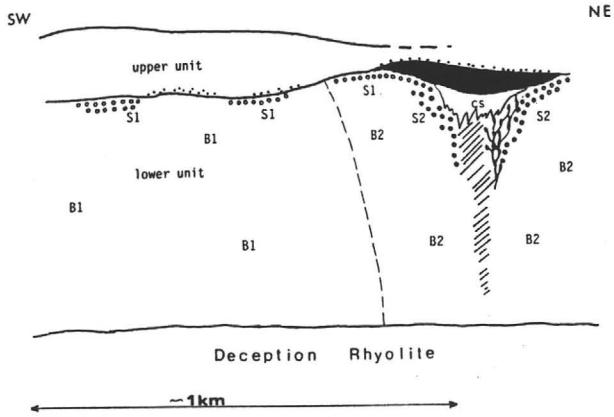

FIG. 3. Interpretative cross section of the Cleopatra Member constructed to show the spatial distribution of alteration types prior to deformation. Sediments deposited at the base of the upper unit are denoted by the stippled pattern. Other patterns are the same as in Figure 2. See Table 2 for description of alteration types.

rather than effects of later deformation and metamorphism, primarily because the brecciated texture diminishes with depth in the main pipe.

The stockwork zone is directly adjacent to the main pipe and it embodies silicified and chloritized blocks of the lower unit separated by sinuous chlorite veins up to 20 cm wide. Minor sulfide mineralization is present within this zone. Monazite is present in the chloritized veins surrounding the altered blocks.

Alteration of the H type is volumetrically most important in the upper unit. It also is found in limited areas of outcrop at the tops of the upper unit and the Deception Rhyolite. Alteration mineralogy consists of the assemblage quartz + albite + hematite ± sericite ± calcite ± relatively Fe-rich chlorite (avg $Fe_{(total)}/Fe_{(total)} + Mg = 0.57$) ± epidote (Table 2). Hematite occurs as veins, as a component of chert veins, and as disseminations throughout the rock groundmass.

Much of the alteration designated as H in the upper unit is characterized by volcaniclastic rocks in which irregularly shaped pink clasts lie in a greenish-gray matrix. The boundaries between clasts and matrix are diffuse, giving the rock a mottled appearance. Clasts and matrix are distinguished on the basis of dominant alteration minerals present and the degree of preservation of phenocrysts. The clasts have a matrix of quartz and sericite, and the quartz and albite phenocrysts are fairly well preserved. The groundmass for the clasts consists predominantly of fine-grained quartz and lesser sericite, and crystal fragments are partially replaced by fine-grained quartz. Hematite, carbonate, chlorite, and epidote are present in both domains. Some of the clasts in the mottled rock contain hematite veins that terminate at the boundary with the silicified matrix. These textural relations suggest pre- and post fragmentation periods of alteration.

Ore Mineralogy

Epigenetic and syngenetic ores are present at the United Verde mine. Epigenetic mineralization occurs in the chlorite schist zone of C-type alteration and in areas of S2-type alteration where it is juxtaposed against the massive sulfide body. The latter was referred to as "quartz porphyry ore" by Anderson and Creasey (1958, p. 123).

Pyrite, chalcopyrite, and sphalerite, the most abundant sulfide minerals, are associated with trace amounts of galena, tetrahedrite, tennantite, and arsenopyrite. In the syngenetic ore, pyrite is the most abundant sulfide. Specularite was noted by Reber (1938) as locally intergrown with pyrite and quartz in the syngenetic ore and by Anderson and Creasey (1958) as occurring in veins that cut chalcopyrite and sphalerite mineralization. Magnetite was found in sulfide interlayers in sediments adjacent to the orebody.

Figure 4, modified from Eastoe and Nelson (1988), depicts the stability relationships for Fe- and Cu-bearing minerals deposited in the United Verde chlorite schist, stockwork zone, and massive sulfide on a log a_{H_2S} versus log a_{O_2} plane. Under the parameters specified (Fig. 4), the stability field of the ore-forming fluid lies within the chalcopyrite field and is further constrained by the contours for $m\Sigma Zn$ in the fluid and the contours of X_{FeS} in sphalerite. The $m\Sigma Zn$ contours are plotted by calculating the molality of zinc as the sum of zinc chloride complexes. A minimum $m\Sigma Zn$ of 10^{-5} was assumed necessary to precipitate a significant amount of sphalerite from the hydrothermal fluid (cf. Anderson, 1977; Ohmoto et al., 1983). The X_{FeS} contours were calculated using an activity coefficient of 2.4 for FeS in sphalerite (Barton and Toulmin, 1968). The mole fractions of FeS in sphalerite from the chlorite schist and the massive sulfide orebody, measured by microprobe analyses of several thin sections, are 0.01 ± .05 and 0.1 ± .05, respectively. These parameters constrain the mineralizing fluid as having a log a_{H_2S} between −5.0 and −2.6, and a log a_{O_2} between −41.7 and −35.5. These values are similar to those estimated for the mineralizing fluid associated with kuroko ore deposition by Ohmoto et al. (1983) and with mineralization at the Permian Afterthought-Ingot area, California (Eastoe and Nelson, 1988). However, the log a_{O_2} is lower than the value of −29.8 calculated for the 350°C solutions being emitted at 21° N, East Pacific Rise (Janecky and Seyfried, 1984) and lower than the range of −35 to −33 estimated for fluids necessary for massive sulfide ore deposition by Dickson (1977).

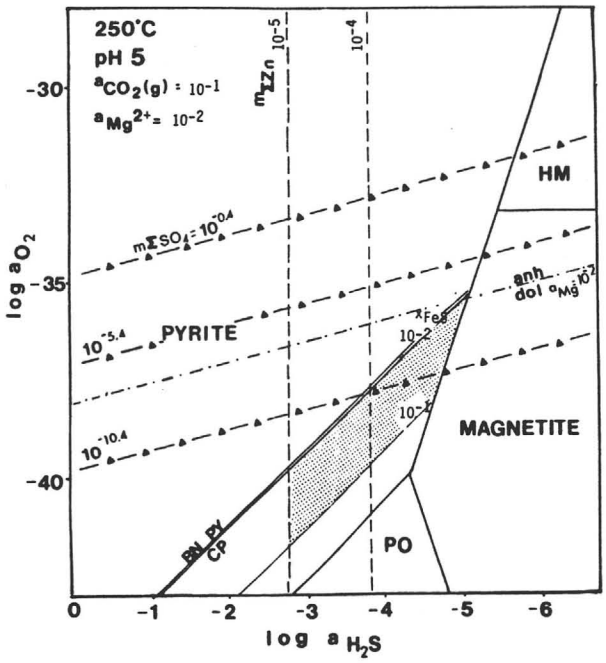

FIG. 4. Diagram of log a_{H_2S} $a_{H_2S_{(aq)}}$ versus log a_{O_2} showing the stability region (stippled) of the hydrothermal fluid responsible for massive sulfide and chlorite schist formation. Conditions assumed other than those listed in the figure include partial pressure of water vapor at 50 bars (Haas, 1976), 0.5 *m* NaCl solution 90 percent disassociated, and a fluid saturated with pyrite (cf. Ohmoto et al., 1983). Thermodynamic data are from Barner and Scheuerman (1978); data on Zn complexes are from Ohmoto et al. (1983); data for $NaSO_4^-$ are from Ohmoto (1972). Activity coefficients were calculated using the modified Debye-Huckel equation of Helgeson (1969); å represents a size parameter for the ionic species of interest, estimated from Garrels and Christ (1965). Standard states for solids are pure crystalline substances at pressure and temperature of interest; standard states for dissolved species are hypothetical ideal 1 *m* solutions at pressure and temperature of interest; standard states for gasses are hypothetical ideal gasses at 1 bar and temperature of interest. Abbreviations: anh = anhydrite, BN = bornite, CP = chalcopyrite, dol = dolomite, HM = hematite, Mg = magnetite, $m\Sigma$ = molarity sum, PO = pyrrhotite, PY = pyrite.

The presence of magnetite in association with pyrite in sediment layers at the edge of the massive sulfide orebody suggests a lower log a_{H_2S} in the hydrothermal fluid at the periphery of the massive sulfide orebody. Hematitic chert and hematite-bearing sediment above the orebody, along with hematitic alteration of the upper unit, suggest a higher a_{O_2} in fluids that postdated those responsible for ore deposition.

Whole-Rock Geochemistry

Methods

Major element oxides, together with loss on ignition, Zr, Nb, and Y were measured by XRAL Laboratories in Don Mills, Ontario, Canada (Table 3; Fig. 5). All analyses were determined by wavelength dispersive X-ray fluorescence spectrometry on a fused disk, except for Y, Nb, and Zr, which were analyzed on pressed pellets. The analytical precision is ±0.01 wt percent for oxides, ±2 ppm for Y and Nb, ±3 ppm for Zr, and ±10 ppm for all other trace elements.

Whole-rock geochemistry

Trace element plots, utilizing the method of Finlow-Bates and Stumpfl (1981), to test for element immobility in all samples of the Cleopatra Member were generated using TiO_2, Al_2O_3, Zr, Nb, and Y. Plots utilizing TiO_2, Al_2O_3, and Zr in pairs yield linear arrays (Fig. 6), suggesting that those elements remained immobile during hydrothermal alteration and metamorphism of the Cleopatra Member. Vance and Condie (1987) also found that TiO_2 remained relatively unchanged in zones of alteration immediately beneath the orebody and used it to monitor qualitatively major element changes. On plots utilizing Al_2O_3, two sample points consistently deviate radically from the array (Fig. 6). These samples represent the chlorite schist zone of type-C alteration. Their deviation suggests that aluminum was added to rocks that are completely chloritized. Interelement ratios utilizing Nb and Y were inconsistent in samples that were chloritized. Lesher et al. (1986) indicated that Y was mobile in the Cleopatra Member during alteration.

The Cleopatra Member is interpreted to represent a series of flows and tuffs produced from one magma chamber. The best evidence is the homogeneous lithologic appearance of both units and immobile element ratios that do not suggest fractionation (cf. Finlow-Bates and Stumpfl, 1981). The Winchester-Floyd discrimination diagram shown in Figure 7 also supports this contention in that all samples from the Cleopatra Member, regardless of degree of alteration, cluster along and just below the boundary between the rhyolite and rhyodacite-dacite fields.

The method of Gresens (1967), which utilizes immobile elements, rock-specific gravities, and calculated volume changes was used to establish major element fluctuations accompanying hydrothermal alteration. In Gresens' method, volume factors are calculated for each altered rock relative to an unaltered equivalent. Volume factors, which represent the change in volume a rock has experienced as a result of alteration, were calculated for each rock utilizing elements considered to be immobile, in this case Al_2O_3, TiO_2, and Zr. Once the volume factor is calculated, major element losses and gains may be calculated using the equation $A(fv\ (g_a/g_u)\ C^i_a - C^i_u) = X^i$, where C is the amount of component i, X is the loss or gain of that component, fv is the volume factor for a particular sample, g is the rock specific gravity, u designates unaltered rock, and a designates altered rock. A is an arbitrary factor which in this case is equal to 100 because of the utilization of whole-rock analyses that total 100 percent.

TABLE 3. Geochemistry (in wt % and ppm) of Select Samples from the Cleopatra Member

Rock	Fe_2O_3*

TABLE 3. Geochemistry (in wt % and ppm) of Select Samples from the Cleopatra Member

Alteration type	Sample no.	SiO_2	TiO_2	Al_2O_3	Fe_2O_3	MnO	MgO	CaO	Na_2O	K_2O	P_2O_5	Loss on ignition	Total	Rock specific gravity	Y	Zr	Nb	$Fe_2O_3^*/Fe_2O_3^* + MgO$	Vol fac	Std dev
Lower unit																				
B1	157	72.5	0.19	12.50	2.14	0.02	2.53	0.96	1.32	4.20	0.04	3.39	99.9	2.75	36	200	12	0.46	0.96	0.11
	75	71.7	0.17	11.70	2.95	0.05	7.24	0.09	0.83	1.31	0.04	4.08	99.6	2.61	50	200	12	0.29	1.07	0.14
	354	63.5	0.21	14.50	5.56	0.04	7.93	0.16	0.09	3.31	0.04	4.47	99.9	2.75	38	210	12	0.41	0.87	0.1
	200	67.9	0.20	13.30	5.42	0.03	4.11	1.16	1.38	2.34	0.04	3.00	99.9	2.74	53	180	12	0.57	0.96	0.12
B2	50	77.2	0.18	11.70	3.62	0.06	2.21	0.01	0.12	2.38	0.04	2.66	100.3	2.73	48	180	12	0.62	1.04	0.12
	42	78.3	0.17	10.60	4.20	0.02	2.47		0.18	1.87	0.02	2.62	100.5	2.72	36	160	10	0.63	1.14	0.13
	47b	78.3	0.15	11.20	2.75	0.03	2.16	0.03	0.05	2.53	0.03	2.31	99.8	2.71	56	190	12	0.56	1.12	0.17
	49	77.5	0.15	8.66	6.72	0.07	3.38	0.03	0.08	0.95	0.03	2.70	100.4	2.73	49	150	10	0.67	1.3	0.17
	47a[1]	65.9	0.11	10.30	11.90	0.09	6.89	0.04	0.09	0.06	0.03	4.47	99.9	2.82	94	140	12	0.63	1.36	0.26
	286	77.3	0.12	8.34	5.36	0.06	4.26	0.05	0.01	0.86	0.03	3.08	99.5	2.72	58	150	12	0.56	1.43	0.21
	102	71.6	0.17	10.90	7.19	0.08	4.36	0.04	0.14	1.39	0.04	3.47	99.5	2.79	56	170	12	0.62	1.08	0.12
	39[1]	53.0	0.22	14.30	14.90	0.07	10.60	0.03	0.13	0.05	0.04	6.47	99.9	2.82	60	210	16	0.58	0.84	0.09
S1	270	77.4	0.19	12.30	1.37	0.01	3.18	0.01	0.15	2.76	0.04	2.85	100.4	2.67	38	200	12	0.30	0.99	0.12
	476	76.4	0.19	12.50	2.23	0.03	0.60	0.11	0.23	5.68	0.04	1.85	100.0	2.63	40	190	12	0.79		
	490	79.6	0.19	12.30	1.10	0.02	0.26	0.08	0.12	4.24	0.04	1.77	99.9	2.62	30	180	12	0.81		
S2	UV-21	74.3	0.23	14.60	1.57	0.01	0.51	0.03	0.11	4.42	0.02	3.70	99.6	2.73	52	230	12	0.75	0.82	0.09
	143	82.6	0.16	9.36	1.62	0.00	1.08	0.00	0.11	2.24	0.02	2.08	99.3	2.68	32	160	12	0.60	1.24	0.16
	UV-3	81.8	0.16	10.40	1.27	0.01	0.29	0.03	0.30	2.65	0.03	2.39	99.4	2.71	28	160	10	0.81	1.18	0.13
	484	73.3	0.19	12.10	4.79	0.03	3.52	0.05	0.20	2.14	0.03	3.62	100.1	2.73	54	180	12	0.58	1.01	0.12
	UV-36	79.6	0.17	12.20	0.83	0.02	1.23	0.06	0.06	3.35	0.04	2.08	99.7	2.70	36	180	12	0.40	1.06	0.13
C	483	25.8	0.15	21.90	23.70	0.15	16.60	0.04	0.05	0.04	0.07	10.10	98.6	2.89	88	100	12	0.59	1.46	0.52
	UV-14	39.0	0.07	16.70	18.40	0.20	14.30	1.51	0.00	0.05	0.12	9.77	100.2	2.86	39	140	12	0.56	1.89	0.8
	31	75.7	0.08	6.40	8.10	0.04	4.52	0.03	0.00	0.03	0.02	3.00	98.6	2.77	24	69	6	0.64	2.47	0.4
	UV-17	77.7	0.12	7.09	6.62	0.05	4.71	0.04	0.02	0.29	0.02	2.93	99.6	2.71	40	120	10	0.58	1.63	0.2
Upper unit																				
	275	71.3	0.21	14.00	2.39	0.03	1.93	2.00	2.90	1.80	0.05	3.62	100.4	2.63	56	220	14	0.55		
	491	75.3	0.18	11.50	2.75	0.04	1.30	1.64	1.53	2.83	0.04	3.00	100.3	2.65	44	160	10	0.68		
H	230	82.0	0.16	9.68	0.83	0.02	0.17	0.86	4.56	0.69	0.04	1.00	100.1	2.63	52	160	10	0.83	1.25	0.15
	127[2]	81.6	0.13	8.35	1.39	0.02	1.23	1.44	1.85	1.30	0.04	2.47	99.9	2.67	40	140	10	0.53	1.44	0.17
	205[2]	75.6	0.16	10.30	1.80	0.04	0.54	3.24	4.79	0.50	0.04		100.1	2.67	34	170	10	0.77	1.18	0.14
	32[3]	72.6	0.21	13.60	2.49	0.04	0.73	2.59	2.70	2.38	0.04	2.85	100.4	2.59	52	200	10	0.77	0.96	0.11
	89[3]	73.8	0.20	12.60	2.64	0.02	1.74	1.11	2.56	2.30	0.04	2.62	99.7	2.70	60	170	20	0.60	1.01	0.13

[1] Samples from chlorite veins
[2] Pervasively hematized samples
[3] Mottled rock
Abbreviations: $Fe_2O_3^*$ = total iron, vol fac = volume factor, calculated according to method of Gresens (1967), Std dev = standard deviation

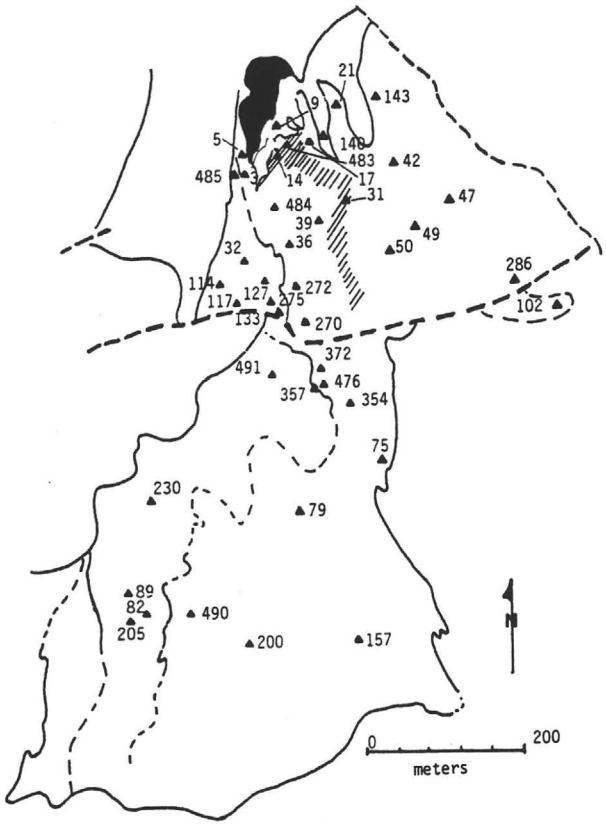

FIG. 5. Location of samples analyzed by microprobe and XRF.

In this study, two least altered samples taken from the upper unit were chosen to represent the least altered Cleopatra Member. They were selected on the basis of chemical composition within the range of average rhyolites and dacites (LeMaitre, 1976), whole-rock oxygen isotope values within the range of rhyodacitic rocks (Taylor, 1968; Gustin et al., in prep.), relatively unaltered feldspar phenocrysts, and a location at least 200 m from the United Verde orebody. Average volume factors were calculated for each altered sample utilizing the three immobile elements and each of the two least altered samples, yielding a value that was an average of six factors (Table 3). Mass balance equations representing average major element oxide changes associated with each of the six alteration types are presented in Table 4.

Grant (1986) rearranged Gresens' equation into a linear relationship between the concentration of components in altered rock and those in the original rock. Those elements exhibiting no loss or gain will define a line called an isocon which intersects the origin. Figure 8 is an isocon diagram (Grant, 1987) for the average least altered upper unit samples versus three least altered lower unit samples from the area of B1-type alteration. In the figure, TiO_2, Al_2O_3, and Zr define the isocon. Those elements and oxides that plot above the line were added to the lower unit; those below were removed. The percent loss and gain of each component may be read off the scale within the diagram. For example, 35 percent K_2O has been added to rocks of the B1 type relative to the least altered Cleopatra Member. The diagram demonstrates that samples from B1-type alteration have higher average abundances of MgO, $Fe_2O_{3(total)}$, and K_2O, slightly less SiO_2, and much less Na_2O and CaO relative to upper unit samples.

Major oxide changes accompanying alteration of most samples from B2-type alteration are represented

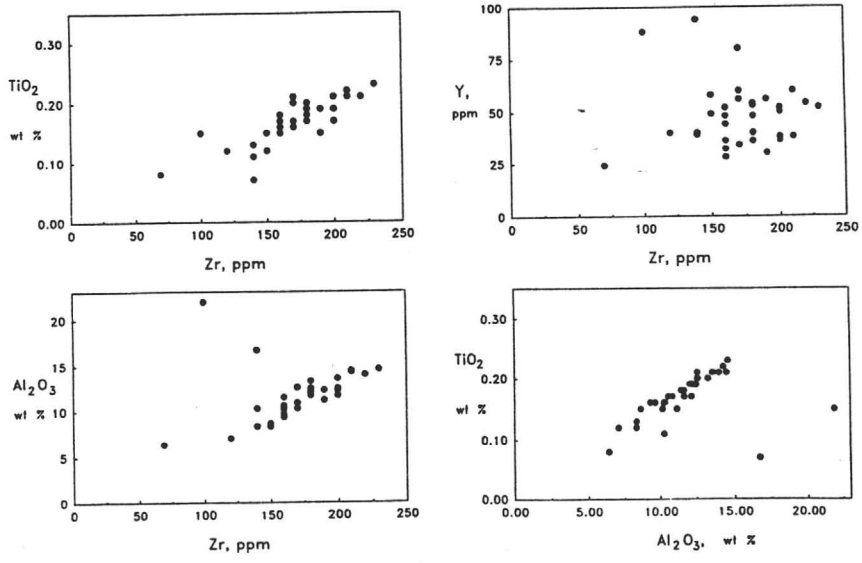

FIG. 6. X-Y plots of elements used to compare component ratios.

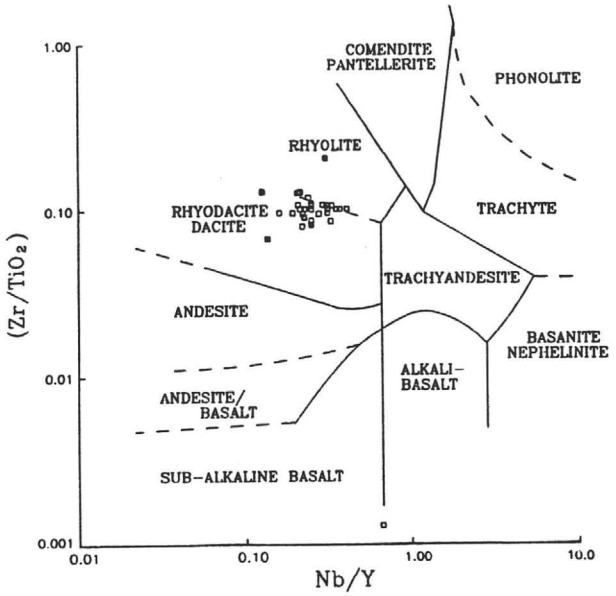

FIG. 7. Plot of Zr/TiO2 vs. Nb/Y, with boundaries from Floyd and Winchester (1978). Analyses from Cleopatra Member. Filled squares represent completely chloritized Cleopatra Member.

by equation (2) of Table 4. Samples from the area of B2-type alteration have 35 percent more iron and 40 percent less CaO and Na_2O than those from the area of B1-type alteration.

Addition of SiO_2 and K_2O, and loss of all other major element oxides except Al_2O_3, are typical of areas of S1- and S2-type alteration. Areas of S2 alteration exhibit the addition of iron and calcium when mineralization is present.

A fourfold increase in MgO and a sevenfold increase in $Fe_2O_{3(total)}$ were calculated for the area of C-type alteration relative to the least altered upper unit samples. In addition, SiO_2 has been added to samples of alteration type C that are not completely chloritized; Al_2O_3 and MnO have been added to samples that are completely chloritized (Table 4). Completely chloritized samples fall into Vance and Condie's (1987) zone 1, in which they documented higher rare earth element (REE) concentrations than other zones and suggested that this may be due to removal of silica accompanying alteration. Petrographic study and verification by EDS microprobe analyses showed that what was once interpreted to be abundant residual zircon in the chlorite pipe is 95 percent monazite and is inferred to have been deposited in the pipe during hydrothermal alteration. This suggests mobilization of the REE from areas surrounding or beneath the chlorite pipe, with subsequent deposition in the chlorite pipe. Lesher et al. (1986) indicated that REE exhibited variable ratios with Zr and were mobile during hydrothermal alteration and metamorphism of the Cleopatra Member. Similar results were documented by Campbell et al. (1984) for the Kidd Creek massive sulfide deposit.

In general, $Fe_2O_{3(total)}/Fe_2O_{3(total)}$ + MgO ratios of whole rocks increase from alteration areas B1 through B2 to the chlorite pipe. Ratios decrease within the chlorite pipe from the base of the main pipe to the chlorite schist zone.

Major element oxide deviations for areas of H-type alteration in the upper unit were estimated using two samples of pervasively hematitized porphyritic rhyodacite and two samples of the mottled volcaniclastic rock. The former has undergone a gain of SiO_2, CaO, and Na_2O, and a loss of MgO and K_2O (Table 4). No enrichment in iron is shown chemically, despite the abundance of hematite (Table 4). No notable gains and losses were calculated for samples of the mottled rock, except for a slight addition of Na_2O. Enrichment of Na_2O has also been demonstrated for

TABLE 4. Mass Balance Equations for Alteration Types of the Cleopatra Member (calculated using the method of Gresens, 1967)

Equation 1: alteration type B1

100 g lauu[1] + 1.15 g Fe_2O_3° + 1.64 g MgO + 0.87 g K_2O = 97.3 g altered rock + 0.78 g CaO + 0.89 g Na_2O + 4.66 g SiO_2

Equation 2: alteration type B2

100 g lauu + 14.4 g SiO_2 + 1.03 g MgO + 1.85 g Fe_2O_3° = 112.67 g altered rock + 1.79 g CaO + 2.04 g Na_2O + 0.78 g K_2O

Equation 3: alteration types S1 and S2

100 g lauu + 23 g SiO_2 + 0.7 g K_2O = 117.46 g altered rock + 1.77 g CaO + 0.83 g MgO + 1.99 g Na_2O + 1.65 g Fe_2O_3

Equation 4: alteration type C (chloritized rocks from deep within the main pipe and from the stockwork zone)

100 g lauu + 52.84 g SiO_2 + 4.99 g MgO + 8.27 g Fe_2O_3° = 161.11 g altered rock + 1.54 g CaO + 2.13 g Na_2O + 1.32 g K_2O

Equation 5: alteration type C (chloritized samples from the chlorite schist and the main pipe immediately beneath the chlorite schist)

100 g lauu + 14.7 g Al_2O_3 + 20.5 g MgO + 27.4 g Fe_2O_3° + 0.23 g MnO = 131.42 g altered rock + 25.2 g SiO_2 + 1.2 g CaO + 2.81 g Na_2O + 2.3 g K_2O

Equation 6: alteration type H (pervasively hematitized rhyodacite)

100 g lauu + 31.7 g SiO_2 + 1.3 g CaO + 2.0 g Na_2O = 132.76 g altered rock + 0.39 g MgO + 1.35 g K_2O + 0.5 g Fe_2O_3°

[1] lauu = least altered upper unit, Fe_2O_3° = total iron

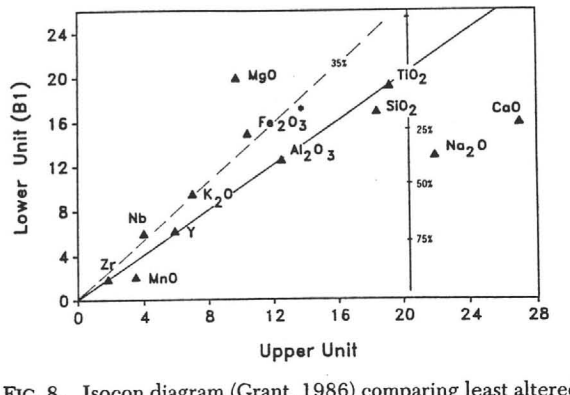

FIG. 8. Isocon diagram (Grant, 1986) comparing least altered upper unit and least altered lower unit samples from alteration type B1. See text for explanation. Major element oxides and trace elements have been multiplied by the following factors in order for all analyses to plot on the same diagram: SiO_2 = wt percent $\times$ 0.25, CaO = wt percent $\times$ 15, MgO = wt percent $\times$ 6, Na_2O = wt percent $\times$ 10, K_2O = wt percent $\times$ 3, $Fe_2O_{3(total)}$ = wt percent $\times$ 4, MnO = wt percent $\times 10^2$, TiO_2 = wt percent $\times 10^2$, Y = ppm $\times$ 10, Zr = ppm $\times 10^{-2}$, and Nb = ppm $\times$ 0.4. Scale on diagram is in either wt percent or ppm, depending upon the element. *indicates total Fe.

the hanging-wall rocks of kuroko-type deposits (Iijima, 1974).

Mineral Chemistry

Methods

The composition of chlorites, sericites, carbonates, plagioclase, and sphalerite were determined using the wavelength dispersive method on the automated ARL electron microprobe of the Department of Earth and Planetary Sciences, University of Arizona. For silicates and sphalerite, analytical conditions were: 15 kV accelerating voltage, 30 nA sample current (0.03 μA), and a 10-μm beam diameter. For carbonates, a 20-μm beam diameter and a 10-nA sample current were used. Intensity data were reduced to concentrations using the program of Bence and Albee (1969). Analytical precision is $\pm$0.5 percent for those oxides having a wt percent of greater than 10, $\pm$0.2 percent for those of 1 to 10 wt percent, and $\pm$0.03 percent for those less than 1 wt percent.

Upper unit versus lower unit mineral chemistry

Variations in mineral chemistry may be used to differentiate between the lower and upper units of the Cleopatra Member. In general, Mn/Mn + Mg + $Fe_{(total)}$ ratios of chlorites, and $Fe_{(total)}/Fe_{(total)}$ + Mg ratios of chlorites and sericites, are higher in the upper unit than in the lower unit (Tables 5 and 6; Fig. 9). Although sericite wt percent totals in Table 6 are low, most likely owing to the fine-grained nature of the material and the presence of interlayers of other phyllosilicates, calculated $Fe_{(total)}/Fe_{(total)}$ + Mg ratios show consistent variation between upper unit and lower unit samples. Similar ratios are reported by Nash (1973).

A plot of $Fe_{(total)}/Fe_{(total)}$ + Mg ratios of coexisting chlorites and sericites displays a fairly linear array (Fig. 10). Sericite and chlorite from upper unit rocks and basal sediments plot slightly above points representing the lower unit phyllosilicates, suggesting that they may have formed in equilibrium with fluids of different chemistry.

Chlorite chemistry

According to the classification of Hey (1954), chlorite from the Cleopatra Member is primarily ripidolite (Fig. 9). Chlorite from basal sediments of the upper unit and B1-type alteration includes the most siliceous variants and is pycnochlorite and clinochlore.

$Fe_{(total)}/Fe_{(total)}$ + Mg ratios of chlorite increase from the area of B1-type alteration to areas of alteration types B2 and C (Fig. 11). Ratios in the chlorite pipe decrease vertically upward toward the inferred sediment-water interface (Fig. 11). Sediments deposited above the orebody have ratios that range from 0.08 to 0.49. Low values correspond to chloritized tuffs and sediments; high values correspond to hematitic cherts and tuffs.

Walshe (1986) developed a solid solution model for chlorite using available thermodynamic data and constraints imposed by measured composition of chlorites from systems where the physicochemical parameters of formation were estimated on the basis of other geochemical data. The model utilizes two geothermometers and the Gibbs-Duhem relation, along with the assumption that the chlorite formed in equilibrium with quartz and an aqueous phase, to calculate the temperature of chlorite formation, the Fe^{+3} value of chlorites, and the mole fraction of Walshe's (1986) sixth thermodynamic component. With these three parameters, other constraints on the chemistry of the chlorite-forming hydrothermal fluid, including a_{O_2}, a_{S_2}, and a_{H_2S}, may be obtained. Walshe et al. (1986) state that fluid parameters calculated at

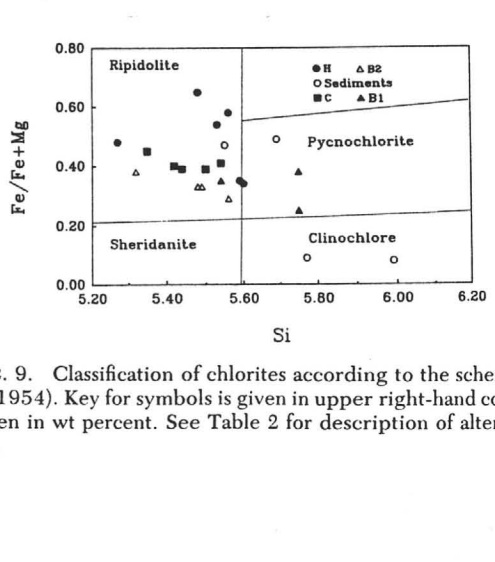

FIG. 9. Classification of chlorites according to the scheme of Hey (1954). Key for symbols is given in upper right-hand corner. Si given in wt percent. See Table 2 for description of alteration types.

temperatures of less than 300°C are underestimated and that temperature estimates are ±20° to 30°C. Problems with Walshe's (1986) solid solution model include the assumption of a value for Fe^{+3} for some chlorites, upon which the model is based, and possible errors in estimated physicochemical conditions of formation of those chlorites, also used as a basis for the model. Some results of the solid solution modeling are given in Table 5.

The log a_{O_2} and log a_{H_2S} values calculated for chlorites from the chlorite pipe using Walshe's model are −33 to −38 and −3.35 to −3.45, respectively. Both are within the range predicted by ore mineral equilibria (Fig. 4). J. L. Walshe (pers. commun., 1986) believes that the Fe^{+3} values calculated using his model are overestimated. Despite the fact that estimated Fe^{+3} values based on stoichiometry (Table 5) differ from those calculated according to the solid solution model, both Fe^{+3} values are highest in chlorites from the area of B1-type alteration.

Calculated temperatures of chlorite formation generally increase laterally from the area of B1-type alteration to the chlorite pipe (Fig. 11). The 252°C temperature calculated for one sample in the area of B1-type alteration was obtained from a chloritized coarse-grained volcaniclastic rock. The high temperature and alteration of the sample suggests that it may have been a part of a fluid conduit. Highest temperatures of formation were calculated for chlorites from the base of the chlorite pipe and from chlorites from veins in B2-type alteration well below the massive sulfide orebody (Fig. 11).

Cathelineau and Nieva (1985) used chlorites to develop an alternative geothermometer based on a strong correlation between aluminum in the tetrahedral site and the temperature of chlorite formation, and the number of vacancies in the octahedral site versus temperature. They derived their geothermometer by comparing microprobe analyses of chlorites with formation temperatures estimated from fluid inclusions and actual temperature measurements from the Los Azufres geothermal system. Velde and Medhioub (1988) suggested that aluminum content is a more reliable indicator of temperature variation compared with other compositional parameters but noted that precursor rock types may also influence Al content. Cathelineau and Nieva (1985) indicated that their equations must be used with caution because other unrecognized intensive and extensive variables may explain the compositional variation.

Temperatures estimated using Cathelineau and Nieva's correlation equations are 20° to 40°C higher than temperatures calculated by Walshe's model. However, both sets of calculated temperatures show the same basic distribution trends which are similar to those expected of massive sulfide systems (cf. Pisutha-Arnond and Ohmoto, 1983). In general, temperatures increase from the area of alteration type B1 to B2 to the base of C and then decrease within the chlorite pipe toward the seawater-rock interface (Fig. 11). Although the temperatures are somewhat lower than those found at active sea-floor spreading centers, the spatial variations are consistent with the interpretation that chlorites were formed during hydrothermal alteration and were not homogenized or significantly modified during the greenschist facies metamorphic event.

Carbonate mineralogy

Carbonate mineralogy was determined using electron microprobe analyses (Gustin, 1988). Carbonate minerals have a distinct spatial distribution in the lower unit. Calcite is characteristic of areas of B1- and S1-type alteration south of the Hull fault, whereas the area of B2-type alteration contains no carbonate minerals. S1-type alteration north of the Hull fault contains dolomite. Magnesium-rich ankerite is the carbonate in veins of exposures of S2- and C-type alteration.

Carbonate mineral distribution in and surrounding the chlorite pipe is postulated to reflect the spatial variation in the chemistry of the hydrothermal fluid. Mg-rich ankerite, found at the top of the main pipe and in alteration type S2, is interpreted to have been deposited from an Fe- and Mg-rich fluid which produced alteration type C and the orebody. Dolomite in S1 alteration and the orebody may have resulted from Fe depletion in the fluid resulting from deposition of iron sulfides in the massive sulfide deposit. Calcite in the distal area of B1-type alteration in the lower unit was most likely a product of low-temperature seawater-rock alteration.

Discussion

Although the greenschist facies metamorphic overprint has changed mineral assemblages, the general geochemical trends associated with the ore-forming system were preserved. Differences in the distribution of alteration types, and in rock and mineral chemistry, are used to distinguish rocks of the stratigraphic hanging wall from those of the footwall to the United Verde ore horizon. They also serve to document recharge versus discharge areas for the hydrothermal fluid and to allow for interpretation of some physical and chemical parameters of the hydrothermal system.

Upper unit versus lower unit

The two units of the Cleopatra Member are distinguished primarily on the basis of alteration types, although lithologic and petrographic differences are present. Hematitized, silicified, and relatively unaltered rocks characterize the upper unit, whereas chloritic and sericitic alteration characterize the lower

TABLE 5. Electron Microprobe Analyses of Chlorite Along with Parameters of

	Upper unit						Basal sediments upper unit				Lower unit: Chlorite schist		Lower unit: Stockwork
Sample no.	240	117	32	114	82	133	4500	458	357	140	UV-9	480	17
Number of analyses	9	5	5	4	4	3	3	3	8	8	3	6	5
SiO_2	27.82	24.80	25.06	26.45	25.27	25.24	25.89	31.36	26.97	29.90	26.45	26.64	26.35
TiO_2	0.02	0.08	0.05	0.01	0.21	0.04	0.00	0.00	0.05	0.06	0.00	0.04	0.04
Al_2O_3	23.43	20.70	21.49	22.01	21.22	22.60	22.22	24.16	20.45	26.37	21.85	23.92	23.04
FeO* [1]	17.29	30.93	24.89	16.17	26.55	24.95	22.22	3.80	24.83	3.98	19.74	19.10	19.12
MnO	0.34	0.48	0.33	0.26	0.30	0.19	0.06	0.23	0.14	0.06	0.12	0.13	0.11
MgO	17.92	9.37	12.07	17.60	10.89	14.92	13.56	24.86	14.36	23.56	17.61	16.92	16.55
Total	86.82	86.35	83.88	82.49	84.44	87.94	83.95	84.41	86.79	83.93	85.76	86.75	85.22
Molecular proportions based on 28 oxygens													
Tetrahedral cations													
Si	5.59	5.48	5.53	5.60	5.56	5.27	5.55	5.99	5.69	5.77	5.50	5.44	5.50
Al	2.39	2.52	2.47	2.52	2.44	2.73	2.46	2.10	2.31	2.23	2.50	2.51	2.50
Octahedral cations													
Al	3.18	2.88	2.97	3.10	3.07	2.84	3.26	3.42	2.75	3.74	2.86	3.25	3.16
Ti	0.00	0.16	0.01	0.00	0.00	0.01	0.00	0.00	0.01	0.01	0.00	0.01	0.01
Fe	2.92	5.72	4.64	2.87	4.89	4.36	3.93	0.61	4.39	0.64	3.44	3.26	3.33
Mn	0.06	0.09	0.20	0.04	0.06	0.03	0.01	0.04	0.03	0.01	0.02	0.02	0.02
Mg	5.39	3.09	3.90	5.56	3.57	4.65	4.40	7.08	4.52	6.79	5.46	5.15	5.14
Total	11.55	11.93	11.71	11.58	11.59	11.89	11.60	11.15	11.70	11.20	11.78	11.69	11.66
Fe/Fe + Mg	0.35	0.65	0.54	0.34	0.58	0.48	0.47	0.08	0.49	0.09	0.39	0.39	0.39
Mn/Mn + Mg + Fe	0.76	1.00	2.26	0.51	0.66	0.37	0.14	0.52	0.29	0.14	0.23	0.27	0.23
Fe^{+3} [2]	0.11	−0.22	0.07	0.27	0.18	0.11	−0.01	0.38	0.16	0.09	0.07	−0.13	0.03
Fe^{+3}/Fe^{*}	0.04	−0.04	0.01	0.09	0.04	0.03	0.00	0.62	0.04	0.15	0.02	−0.04	0.01
Parameters calculated by J. L. Walshe and B. P. Harrold (pers. commun., 1986)													
Fe^{+3}	0.27		0.39	0.27	0.39	0.41	0.34	0.07	0.36	0.07	0.32	0.31	0.31
Fe^{+3}/Fe^{*}	0.09		0.08	0.10	0.08	0.09	0.09	0.11	0.08	0.11	0.09	0.09	0.09
Temperature (°C)	228.30		249.00	230.10	238.70	291.80	239.20	179.40	221.00	210.40	254.20	256.90	249.30
Log a_{O_2}	−38.10		−38.30	−37.80	−40.20	−32.30	−38.70	−36.80	−41.70	−32.00	−35.60	−35.00	−36.10
Log a_{H_2S}									−3.21		−3.34	−3.39	−3.40

[1] FeO* and Fe* represent total iron
[2] Fe^{+3} estimated based on stochiometry

unit. The upper unit contains a higher percentage of volcaniclastic rocks than the lower unit and lacks the polycrystalline quartz grains that typify the groundmass of the lower unit.

All samples of the lower unit are enriched in MgO and depleted in alkalies relative to least altered upper unit samples. In contrast, altered upper unit samples are enriched in alkalies. The presence of hematite, excess silica, and relatively Fe-rich phyllosilicates, and the preservation of albite suggest that the upper unit equilibrated with a silica-saturated fluid of alkaline or neutral pH that was more oxidized relative to the ore-forming fluid. In contrast, the lower unit equilibrated with an Mg- and Fe-rich fluid that was reducing and slightly acidic, as evidenced by the depletion of alkalies and the stability of sericite and chlorite. The lower unit is interpreted to have been altered by an evolving ore-forming hydrothermal fluid, assumed to have been seawater that was modified progressively through water-rock interaction. Upper unit alteration postdated ore deposition and was produced by interaction with a geochemically distinct fluid that may represent subsea-floor metamorphism (cf. Harper et al., 1988; Zierenberg et al., 1988), perhaps associated with the waning stages of the hydrothermal system.

Alteration of the lower unit

Major element distribution trends from the area of B1 to C alteration include progressive removal of CaO and Na_2O, increasing additions of $Fe_2O_{3(total)}$ and MgO, and increasing values for iron to iron plus magnesium ratios of whole rocks and chlorites (Fig. 12). These geochemical variations are typical of traverses in the stratigraphic footwall of other massive sulfide deposits from relatively unaltered rocks at some distance from the orebody to altered rocks immediately beneath the

Chlorite Formation Calculated Using Walshe's (1986) Solid Solution Model

Main pipe		B2-type alteration					B1-type alteration			Mescal gulch	Verde Central mine
482	31	39	102	143	47	42	372	354	200		
9	11	6	10	5	8	4	5	4	8	6	11
26.64	26.15	26.23	25.87	27.63	26.27	26.27	27.02	28.93	27.20	26.76	27.11
0.03	0.03	0.04	0.04	0.04	0.05	0.00	0.05	0.04	0.08	0.33	0.06
22.00	22.92	22.61	22.84	22.43	23.51	24.09	19.91	20.92	21.76	24.41	19.03
20.44	23.55	20.24	21.38	18.00	23.32	22.00	19.00	13.54	19.39	11.81	23.12
0.11	0.12	0.08	0.30	0.11	0.17	0.18	0.14	0.13	0.14	0.06	0.12
16.61	16.20	17.26	14.47	19.39	16.38	13.41	17.43	22.82	18.87	21.73	16.84
85.83	88.96	86.46	84.90	87.59	89.69	85.95	83.53	86.38	87.44	85.11	86.29
5.54	5.35	5.42	5.48	5.56	5.32	5.49	5.75	5.75	5.54	5.36	5.73
2.46	2.65	2.58	2.52	2.45	2.68	2.51	2.25	2.36	2.46	2.64	2.27
2.98	2.84	2.93	3.17	2.93	2.93	3.40	2.75	2.65	2.76	3.13	2.53
0.00	0.00	0.02	0.01	0.00	0.01	0.00	0.01	0.01	0.01	0.05	0.01
3.57	4.03	3.51	3.82	3.03	3.95	3.84	3.38	2.25	3.14	1.98	4.09
0.02	0.02	0.01	0.05	0.02	0.03	0.03	0.02	0.02	0.02	0.01	0.02
5.16	4.95	5.31	4.57	5.82	4.94	4.18	5.53	6.77	5.72	6.49	5.27
11.73	11.84	11.78	11.62	11.80	11.85	11.46	11.69	11.70	11.65	11.67	11.92
0.41	0.45	0.40	0.46	0.34	0.44	0.48	0.38	0.25	0.35	0.23	
0.22	0.21	0.15	0.64	0.21	0.32	0.38	0.27	0.24	0.27	0.13	0.23
0.02	0.13	0.07	0.12	−0.09	0.06	0.19	0.12	0.32	0.40	0.17	−0.08
0.01	0.03	0.02	0.03	−0.03	0.01	0.05	0.04	0.14	0.13	0.09	−0.02
0.32	0.38	0.33	0.33	0.29	0.38	0.33	0.31	0.23	0.31	0.36	0.21
0.09	0.09	0.11	0.09	0.10	0.10	0.09	0.09	0.10	0.10	0.18	0.05
242.10	280.20	248.90	265.60	244.80	284.30	244.90	210.60	217.10	252.00	225.40	277.60
−37.50	−33.20	−37.00	−34.30	−36.10	−32.60	−37.70	−41.50	−38.20	−35.70	−40.60	−29.60
−3.35	−3.02	−3.22	−3.26	−3.55	−3.03						

orebody (Franklin et al., 1981; Costa et al., 1983; Green et al., 1983; Urabe et al., 1983). These trends are interpreted to reflect changes in hydrothermal fluid chemistry due to fluid-rock interaction and increases in the temperature of the hydrothermal fluid.

The recharge zone for the hydrothermal fluid associated with massive sulfide formation should be characterized by alteration that suggests low-temperature seawater-rock interaction. Experimental work has shown that during the initial stages of seawater-rock reaction, rocks become enriched and seawater becomes depleted in Mg (Dickson, 1977; Mottl and Holland, 1978; Mizukami and Ohmoto, 1983). This exchange increases the acidity of the fluid and the ability of the solution to break down feldspars and volcanic glass, which releases Ca and Na from the rocks. The fluid should also become depleted in carbonate as it reacts with the excess calcium to make calcite (Reed, 1982; Mizukami and Ohmoto, 1983). Pisutha-Arnond and Ohmoto (1983) have defined for kuroko deposits a low-temperature recharge zone (zone b, Fig. 13) which has the geochemical characteristics described above. In their zone b, analcime, calcite, illite, and quartz have been added to rhyodacitic rocks already altered to an assemblage of Mg-Na-type montmorillonite, clinoptilolite, mordenite, saponite, and low cristobalite (Fig. 13).

Geochemical data suggest that alteration type B1 of the lower unit located south of the Hull fault was part of the recharge area for the United Verde ore-forming hydrothermal fluid. This area of alteration is analogous to a metamorphosed zone b of Pisutha-Arnond and Ohmoto (1983). Depletion in alkalies and silica, the presence of calcite, and low $Fe_{(total)}/Fe_{(total)}$ + Mg ratios of rocks and chlorites are evidence for low-temperature seawater-rock interaction (Fig. 12).

TABLE 6. Electron Microprobe Analyses of Sericite

	Upper unit						Lower unit							
	H			Sediments			S2				B2			B1
Alteration type														
Sample no.	240	82	114	32	485	357	36	UV5	143	21	50	372	57	354
Number of analyses	1	4	1	6	5	1	3	4	2	7	3	5	5	3
SiO_2	40.81	45.61	45.97	46.63	44.04	47.73	47.77	46.98	46.39	46.99	46.39	48.87	46.35	41.59
TiO_2		0.23	0.10	0.12	0.03	0.09	0.12	0.12	0.09	0.17		0.27	0.17	
Al_2O_3	30.24	31.44	36.01	32.09	35.97	32.28	33.61	35.78	33.25	35.08	31.59	29.75	30.12	25.40
FeO° [1]	7.96	3.71	2.68	3.58	1.46	3.11	0.39	0.22	0.59	0.45	0.48	2.87	3.00	6.61
MnO	0.14	0.02		0.03	0.06		0.02	0.03	0.04	0.01	7.87	0.04	0.03	0.05
MgO	6.48	0.96	0.80	0.89	5.33	1.27	0.74	0.94	0.84	1.06	0.06	2.33	1.82	11.07
CaO	0.06	0.06	0.12	0.08	0.40	0.01	0.02	0.78	0.07	0.02	3.61	0.07	0.14	0.05
Na_2O	0.49	0.24	1.01	0.44	4.23	0.22	0.05	0.94	0.52	0.49	0.02	0.13	0.34	0.10
K_2O	6.49	10.82	9.78	10.49	2.44	10.49	10.01	9.82	9.90	10.57	4.40	10.89	10.62	6.76
Total	92.67	93.09	96.47	94.35	93.96	95.20	92.73	95.61	91.69	94.84	94.42	95.22	92.59	91.63
Molecular proportions based on 22 oxygens														
Si	5.75	6.13	6.07	6.32	5.92	6.39	6.44	6.22	6.93	6.24	6.59	6.56	6.42	5.90
Al(tet)	2.25	1.87	1.93	1.68	2.08	1.61	1.56	1.78	1.07	1.76	1.41	1.44	1.58	2.10
Al(oct)	2.77	3.26	3.68	3.48	3.57	3.49	3.79	3.80	4.78	4.73	4.30	3.32	3.34	2.17
Fe°	0.94	0.42	0.30	0.41	0.16	0.35	0.04	0.07	0.07	0.13	0.56	0.30	0.35	0.79
Mg	1.36	0.20	0.16	0.18	0.84	0.25	1.46	0.19	0.18	0.21	0.83	0.46	0.38	2.30
Na	0.13	0.20	0.26	0.27	1.12	0.57	0.01	0.24	0.24	0.13	0.12	0.00	0.09	0.04
K	1.17	1.94	1.65	1.83	0.43	1.86	0.86	1.66	1.65	1.79	1.55	1.79	1.88	1.02
Oct(total)	3.74	3.70	3.98	3.89	3.74	3.85	3.83	3.87	4.86	4.87	4.88	3.62	3.73	2.98
Fe/Fe + Mg	0.41	0.68	0.65	0.69	0.16	0.58	0.03	0.27	0.28	0.39	0.40	0.39	0.48	0.26

[1] FeO° and Fe° represent total iron

FIG. 10. I
from sample
unit samples,
= lower unit

Estimated
of alteratio
with a sli
evolved fl
tion types
ratios of
Reardon (
fluid recha
teration al
in the stud
in the fluid
phases at l
been enha
the absorp
et al., 198

The int
progressiv
ward the
culminate
sent the m
fluid. The
the main F

FIG. 11.
$Fe_{(total)}/Fe_{(c}$
formation,
Figure 2 fo

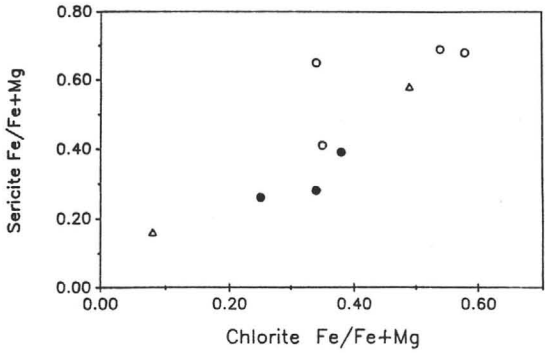

FIG. 10. $Fe_{(total)}/Fe_{(total)}$ + Mg ratios of chlorites versus sericites from samples of the Cleopatra Member. Open circles = upper unit samples, triangles = basal upper unit sediments, filled circles = lower unit samples.

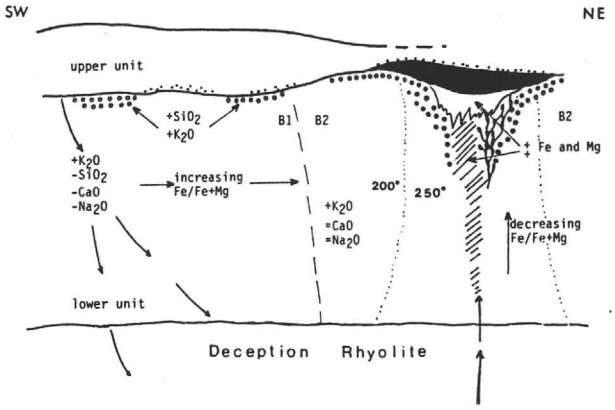

FIG. 12. Diagram summarizing major element losses and gains from alteration types of the lower unit. See Figure 2 for alteration types.

Estimated values of Fe^{+3} for chlorites from this area of alteration are relatively high, suggesting interaction with a slightly more oxidizing and therefore less evolved fluid than that interacting with other alteration types. High Fe^{+3} values and low Fe/Fe + Mg ratios of chlorite were predicted by Roberts and Reardon (1978) for chlorites formed in the area of fluid recharge. Chlorites from the area of B1-type alteration also have the highest silica contents obtained in the study. This may be attributed to silica saturation in the fluid owing to the breakdown of primary silicate phases at low temperatures. Silica solubility may have been enhanced, owing to increased salinity caused by the absorption of water by alteration phases (Fournier et al., 1982; Mizukami and Ohmoto, 1983).

The intensity of hydrothermal alteration increases progressively in the lower unit from Hull Canyon toward the United Verde orebody. Alteration effects culminate in the chlorite pipe, interpreted to represent the main discharge conduit for the hydrothermal fluid. The brecciated nature of the rock at the top of the main pipe, the pervasive replacement of the lower unit by chlorite, and the presence of a large accumulation of massive sulfide directly above this area suggest that this area was a highly permeable zone of fluid discharge. A rough estimate of the amount of fluid discharged through the chloritized pipe can be made by considering the amount of iron deposited in the massive sulfide orebody. Based on calculations by J. L. Walshe and B. P. Harrold (writ. commun., 1987) the log $a_{Fe^{+2}}$ of the fluid associated with chlorites in the chlorite pipe was approximately −3.8. Assuming that $FeCl^-$ was the dominant iron complex in the hydrothermal fluid (cf. Barnes, 1979) and using log K values from Ohmoto et al. (1983), an activity coefficient of 0.366 for $FeCl^-$, and a pH of 5, an estimated 1.52×10^{17} kg of fluid would have been necessary to deposit 85 million tons of pyrite. This figure is a rough approximation of the amount of pyrite deposited in the United Verde orebody. This is a minimum estimate; the iron lost in solution and deposited in other phases is not considered.

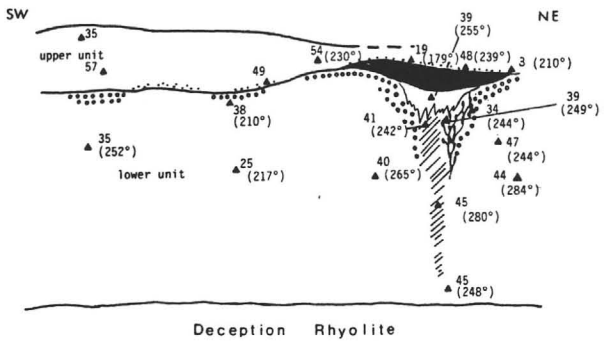

FIG. 11. Schematic cross section showing the distribution of $Fe_{(total)}/Fe_{(total)}$ + Mg ratios of chlorite and temperatures of chlorite formation, calculated using the scheme of Walshe (1986). See Figure 2 for alteration types.

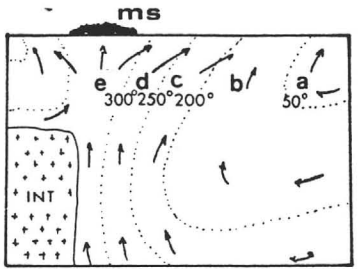

FIG. 13. Diagram summarizing the types of alteration associated with kuroko-type deposits, from Pisutha-Arnond and Ohmoto (1983). Dotted lines represent isotherms with an uncertainty of 50°C. Arrows indicate flow directions for pore fluids. Alteration types: a = clinoptilotite- and mordenite-bearing zeolite zone, b = analcime- and calcite-bearing zeolite zone, c = montmorillonite zone, d = transition zone, e = sericite and chlorite zone; ms = massive sulfide, INT = intrusion.

The zone of exposed B2-type alteration is transitional between the recharge and discharge areas for the hydrothermal fluid. It is very similar geochemically to Pisutha-Arnond and Ohmoto's (1983) zones c and d of alteration associated with kuroko-type deposits (Fig. 13). In their zones c and d, montmorillonites, illites, and sericites are the dominant phyllosilicates; plagioclase is incompletely to completely replaced. At Jerome, plagioclase is completely replaced in samples from alteration type B2. Rocks from this area are more enriched in iron than in magnesium, suggesting interaction with an evolved fluid enriched in iron. This fluid most likely overprinted earlier low-temperature alteration by Mg-rich seawater. Interaction with an acidic fluid undersaturated in Ca and Na is suggested by the removal of Ca and Na, feldspar, and calcite from rocks of this area of alteration (Fig. 12). Thus the area of B2-type alteration was subjected to alteration by low-temperature seawater during the initial stages of the development of the United Verde hydrothermal cell, and to later alteration by an ascending evolved hydrothermal fluid.

Exposures of S1-type alteration are interpreted to be the result of early small circulation cells developed within the lower unit prior to the development of the large cell necessary to form the United Verde deposit (Fig. 14). Small cells are described by Solomon et al. (1987) as forming in the initial stage of development of a convection system in a permeable medium. During the development of small precursor cells in the lower unit, as a result of seawater-rock interaction, Mg^{+2} and OH^- ions would have been removed from seawater, causing the fluid to become somewhat acidic and silica saturated. Fluid in these cells, upon rising toward the interface between the lower unit and seawater, cooled and interacted with the wall rock, resulting in sericitic alteration and silica precipitation.

The area of S2-type alteration surrounding the chlorite pipe is interpreted to have been produced by changing fluid chemistry owing to the deposition of chlorite in the pipe. Upon formation of chlorite, Fe^{+2} and Mg^{+2} are removed from the fluid. The resulting increase in the activity of K^+ would shift the fluid chemistry into the sericite stability field. Larson (1984) proposed the same model for similar zonation of alteration mineralogy at the Proterozoic Bruce deposit of Arizona.

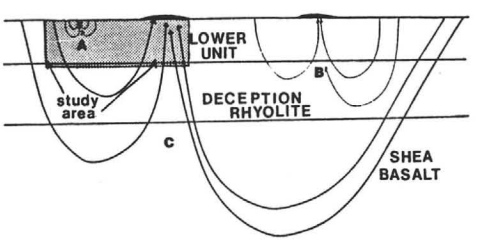

FIG. 14. Schematic cross section showing the size of the study area in relation to the entire United Verde hydrothermal cell. Cell A represents a precursor small cell responsible for alteration type S1. Cell B represents the cell responsible for forming the United Verde Extension orebody. Cell C represents the large cell that produced the United Verde orebody.

Evidence for mixing

Mixing of seawater with the hydrothermal fluid is inferred to have occurred at the top of the main pipe and in the chlorite schist zone on the basis of: decreasing $Fe_{(total)}/Fe_{(total)} + Mg$ ratios of both rocks and chlorites, decreasing temperatures of chlorite formation and increasing silica content of chlorite toward the sediment-water interface, and oxygen isotope evidence (Gustin et al., in prep) for decreasing temperatures toward the sediment-water interface and for mixing of an isotopically distinct hydrothermal fluid with seawater. Roberts and Reardon (1978) and Costa et al. (1983) suggested that magnesium enrichment in the upper level of the discharge pipe at the Mattagami Lake mine could be attributed to the mixing of an ascending acidic ore fluid with seawater immediately beneath the sea floor. Mixing of seawater with the hydrothermal fluid in the upper level of the main pipe would cause the seawater to increase in temperature, facilitating removal of Mg from the seawater. If the fluid was venting rapidly, as suggested by Franklin (1986) for most Cu-Zn deposits with chlorite-rich pipes, cold seawater would be drawn into this zone. Franklin (1986) explained rapid venting as a product of density differences between seawater and the hydrothermal fluid.

Chlorite samples with the highest Fe concentrations, highest calculated formation temperatures, and relatively low silica values are from deep in the chlorite pipe and from veins in the area of B2. These include samples 31, 47a, 39, and a few analyses of sample 102 (Table 5). Chlorites from the chlorite schist zone are more silica rich. This may be a product of mixing of the hydrothermal fluid with cooler seawater in the upper level of the pipe, which would decrease silica solubility in the fluid, or it may reflect higher solubility of quartz in the fluid deep within the chlorite pipe. Kranidiotis and MacLean (1987) explain a similar, but more extreme, distribution of chlorite compositions at the Precambrian Phelps Dodge deposit, Quebec, as a product of increased quartz solubility at high temperatures possibly near the critical point of water (cf. Kennedy, 1950) occurring deep within the pipe.

Source of components, heat source, size of the hydrothermal cell

The presence of ankerite in the upper level of the main pipe necessitates a source of CO_2, assuming that CO_2 in seawater was lost owing to initial water-rock interaction. Fluids rich in CO_2 relative to seawater

are reported from fluid inclusions associated with the area of fluid discharge at kuroko-type deposits (Pisutha-Arnond and Ohmoto, 1983) and were measured from fluids collected from discharge sites at the East Pacific Rise (Janeckey and Seyfried, 1984). Morton and Nebel (1984) summarized several means of enriching a hydrothermal fluid in CO_2 following initial depletion of seawater CO_2 in the area of low-temperature fluid-rock interaction. These include (1) leaching and transporting of diagenetic carbonate, (2) leaching of CO_2 from basalts deeper in the section (Seyfried and Mottl, 1982), and (3) decarbonation reactions occurring during metamorphism deep in the volcanic section concurrent with convection. Another potential source of CO_2 is seawater. If mixing of seawater with a fluid enriched in Ca and Fe occurred in the upper level of the chlorite pipe, it is plausible that carbonate minerals could have been precipitated. All of the above are reasonable; however, carbon isotope data (Gustin et al., in prep) suggest that the CO_2 was derived from diagenetic carbonate in the host rocks.

Neither the Cleopatra Member nor any other unit of the Deception Rhyolite appears to have been the source of the ore metals, iron, or magnesium added to the chlorite pipe and orebody. Neither shows notable depletion in copper or zinc relative to unaltered rhyolites and dacites (Gustin, 1988). Mass balance calculations demonstrate that rocks of the lower unit are enriched in total Fe_2O_3 and MgO. Iron and magnesium were added to the Deception Rhyolite as components in chlorite. If a large part of the seawater Mg was deposited during initial seawater-rock interaction, an additional source of magnesium other than seawater is required.

Below the Deception Rhyolite, the Shea Basalt may have provided the additional CO_2, Fe, Mg, Mn, and metals that enriched the chlorite pipe and the orebody. Mottl et al. (1979) demonstrated that temperatures in excess of 300°C are necessary to derive a significant amount of iron from a basalt. Franklin (1986), citing evidence from sea-floor spreading centers and experimental work, concluded that temperatures must be as high as 385°C and water/rock ratios must be low in order to promote metal leaching. These prerequisite conditions for removal of metals could only have occurred at a stratigraphic level below the Deception Rhyolite.

The study area represents only a small portion of the United Verde hydrothermal cell. Figure 14 is a schematic diagram illustrating the size of the study area in relation to the entire hypothesized United Verde cell. The circulation of the United Verde hydrothermal cell below the Cleopatra Member and the Deception Rhyolite is suggested by the lack of a metal or heat source for the system in either of these units.

Solomon et al. (1987) estimated, on the basis of metal solubilities in ore solutions associated with massive sulfide systems, that catchment areas on the order of 100 km^2 are theoretically required for massive sulfide deposits similar in size to the United Verde deposit. They suggested that this figure could be reduced with an alternative source of metal such as a magmatic component. The largest intrusive body in the area is a granodiorite located approximately 7 km south of the United Verde mine, an unreasonable depth for hydrothermal fluid circulation associated with massive sulfide-forming systems, on the basis of both experimental work (Sleep and Woolery, 1978; Bischoff and Rosenbauer, 1984) and estimates from natural settings (Gregory and Taylor, 1981; Morton and Nebel, 1984; Muehlenbachs, 1986; Polya et al., 1986). It is possible that a mafic sill-dike complex in the Shea Basalt reported by Anderson (1986) may have provided a magmatic component as well as the heat source that drove the hydrothermal system. The Shea Basalt is approximately 2.5 km below the orebody, a much more reasonable depth for hydrothermal fluid circulation. One must not rule out the possibility that a cryptic magma chamber responsible for erruption of the Cleopatra Member contributed a magmatic component.

It is possible, as suggested above, that the United Verde ore-forming fluid interacted with the Shea Basalt and leached Fe, Mg, and ore metals, with little being contributed from a magmatic source. Despite these conjectures, the heat and metal sources still remain enigmas in the history of the United Verde orebody.

Acknowledgments

This research was part of a Ph.D. study at the University of Arizona. The author gratefully acknowledges reviews by C. J. Eastoe, M. M. Gustin, C. M. Lesher, and *Economic Geology* reviewers. Research support was provided by the Anaconda Mining Company, the Santa Fe Mining Company, Sigma Xi, and the Graduate Student Development Fund of the University of Arizona.

Special thanks are due the Phelps Dodge Corporation, and especially Jonathan DuHamel, for use of their maps, thin sections, and drill core from the Jerome area. I greatly appreciate access to their properties in the Verde district and provision of accommodations for myself and my family when in the area.

Much gratitude is extended to M. Drake of the Department of Earth and Planetary Sciences at the University of Arizona for use of the ARL microprobe; and to J. M. Walshe and B. P. Harrold for processing my chlorite data. Paul Lindberg and Dale Armstrong deserve special thanks for introducing me to the area and for stimulating discussions on the geology. Special thanks to all the field assistants who accompanied me to Jerome, especially M. M. Gustin.

September 7, 1988; October 16, 1989

REFERENCES

Anderson, C. A., and Creasey, S. C., 1958, Geology and ore deposits of the Jerome Area, Yavapai County, Arizona: U. S. Geol. Survey Prof. Paper 308, 185 p.

Anderson, C. A., and Nash, J. T., 1972, Geology of the massive sulfide deposits at Jerome, Arizona: A reinterpretation: ECON. GEOL., v. 67, p. 845–863.

Anderson, C. A., Blacet, P. M., Silver, L. T., and Stern, T. W., 1971, Revision of Precambrian stratigraphy in the Prescott-Jerome area, Yavapai County, Arizona: U. S. Geol. Survey Bull. 1324-C, 16 p.

Anderson, G. M., 1977, Thermodynamics and sulfide solubilities: Mineralog. Assoc. Canada Short Course Handbook, v. 2, p. 136–150.

Anderson, P. A., 1986, The Proterozoic tectonic evolution of Arizona: Unpub. Ph.D. dissert., Tucson, Univ. Arizona, 416 p.

Anderson, P. A., and Guilbert, J. M., 1979, The Precambrian massive sulfide deposits of Arizona—a distinct metallogenic epoch and province: Nevada Bur. Mines Rept. 33, p. 29–48.

Barner, H. E., and Scheuerman, R. V., 1978, Handbook of thermochemical data for compounds and aqueous species: New York, Wiley Intersci., 156 p.

Barnes, H. L., 1979, Solubilities of ore minerals, *in* Barnes, H. L., ed., Geochemistry of hydrothermal ore deposits, 2nd ed.: New York, Wiley Intersci., p. 404–406.

Barton, P. B., Jr., and Toulmin, P., III, 1968, Phase relations involving sphalerite in the Fe-Zn-S system: ECON. GEOL., v. 61, p. 815–849.

Bence, A. E., and Albee, A. L., 1969, Microanalysis of silicates and oxides: Jour. Geology, v. 76, p. 382–403.

Bischoff, J. L., and Rosenbauer, R. J., 1984, The critical point and two-phase boundary of seawater, 200–500°C: Earth Planet. Sci. Letters, v. 68, p. 172–180.

Campbell, I. H., Lesher, C. M., Coad, P., Franklin, J. M., Gorton, M. P., and Thurston, P. C., 1984, Rare earth element mobility in alteration pipes below massive Cu-Zn sulfide deposits: Chem. Geology, v. 45, p. 181–202.

Cathelineau, M., and Nieva, D., 1985, A chlorite solid solution geothermometer—the Los Azufres (Mexico) geothermal system: Contr. Mineralogy Petrology, v. 91, p. 235–244.

Costa, U. R., Barnett, R. L., and Kerrich, R., 1983, The Mattagami Lake Mine Archean Zn-Cu sulfide deposit, Quebec: Hydrothermal co-precipitation of talc and sulfides in a sea-floor brine pool: Evidence from geochemistry, $^{18}O/^{16}O$, and mineral chemistry: ECON. GEOL., v. 78, p. 1144–1203.

Dickson, F. W., 1977, The role of rhyolite-seawater reaction in the genesis of Kuroko ore deposits: Internat. Symposium on Water-Rock Interaction, 2nd, Strasbourg, 17–25 August, 1977, Proc., p. iv181–iv190.

Eastoe, C. J., and Nelson, S. E., 1988, A Permian kuroko-type hydrothermal system, Afterthought-Ingot area, Shasta County, California: Lateral and vertical sections, and geochemical evolution: ECON. GEOL., v. 83, p. 588–605.

Finlow-Bates, T., and Stumpfl, E. F., 1981, The behavior of so-called immobile elements in hydrothermally altered rocks associated with volcanogenic submarine exhalative ore deposits: Mineralium Deposita, v. 16, p. 319–328.

Fiske, R. S., and Matsuda, T., 1964, Submarine equivalents of ash flows in the Tokiwa Formation, Japan: Am. Jour. Sci., v. 262, p. 76–106.

Floyd, P. A., and Winchester, J. A., 1978, Identification and discrimination of altered and metamorphosed volcanic rocks using immobile elements: Chem. Geology, v. 21, p. 291–306.

Fournier, R. O., Rosenbauer, R. J., and Bischoff, J. L., 1982, The solubility of quartz in aqueous sodium chloride solution at 350°C and 180-500 bars: Geochim. et Cosmochim. Acta, v. 46, p. 1975–1978.

Franklin, J. M., 1986, Volcanic-associated massive sulphide deposits—an update, *in* Andrew, C. J., Crowe, R. W. A., Finlay, S., Pennell, W. M., and Pyne, J. F., eds., Geology and genesis of mineral deposits in Ireland: Irish Assoc. Econ. Geology, p. 49–69.

Franklin, J. M., Lyndon, J. W., and Sangster, D. F., 1981, Volcanic-associated massive sulfide deposits: ECON. GEOL. 75TH ANNIV. VOL., p. 485–627.

Garrels, R. M., and Christ, C. L., 1965, Solutions, minerals and equilibria: New York, Harper Row Pub., 450 p.

Grant, J. A., 1986, The isocon diagram—a simple solution to Gresens' equation for metasomatic alteration: ECON. GEOL., v. 81, p. 1976–1982.

Green, G. R., Ohmoto, H., Date, J., and Takahashi, T., 1983, Whole-rock oxygen isotope distribution in the Fukazawa-Kosaka area, Hokuroku district, Japan, and its potential application to mineral exploration: ECON. GEOL. MON. 5, p. 395–411.

Gregory, R. T., and Taylor, H. P., Jr., 1981, An oxygen isotope profile in a section of Cretaceous oceanic crust, Samail ophiolite, Oman: Evidence for $\delta^{18}O$ buffering of oceans by deep (>5 km) seawater-hydrothermal circulation at mid-ocean ridges: Jour. Geophys. Research, v. 86, p. 2737–2755.

Gresens, R. L., 1967, Composition-volume relations of metasomatism: Chem. Geology, v. 2, p. 47–65.

Gustin, M. S., 1988, A petrographic, geochemical and stable isotope study of the United Verde orebody and its associated alteration, Jerome, Arizona: Unpub. Ph.D. dissert., Tucson, Univ. Arizona, 261 p.

Hansen, M. G., 1930, Geology and ore deposits of the United Verde Mine: Mining Cong. Jour., v. 16, p. 8–13.

Harper, G. D., Bowman, J. R., and Kuhns, R., 1988, A field, chemical, and stable isotope study of subseafloor metamorphism of the Josephine ophiolite, California: Jour. Geophys. Research, v. 93, pt. B5, p. 4625–4656.

Haas, J. L., 1976, Physical properties of the coexisting phases and thermochemical properties of the H_2O component in boiling NaCl solutions: U. S. Geol. Survey Bull. 1421-A, 47 p.

Helgeson, H. G., 1969, Thermodynamics of hydrothermal systems at elevated temperatures and pressures: Am. Jour. Sci., v. 267, p. 729–804.

Hey, M. H., 1954, A new review of the chlorites: Mineralog. Mag., v. 30, p. 277–292.

Iijima, A., 1974, Clay and zeolitic alteration zones surrounding Kuroko deposits in Hokuroku district, Northern Akita, as submarine hydrothermal-diagenetic alteration products: Soc. Mining Geologists Japan Spec. Issue 6, p. 267–290.

Janecky, D. R., and Seyfried, W. E., Jr., 1984, Formation of massive sulfide deposits on ocean ridge crests: Incremental reaction models for mixing between hydrothermal solutions and seawater: Geochim. et Cosmochim. Acta, v. 48, p. 2723–2738.

Karlstrom, K. E., Bowring, S. A., and Conway, C. M., 1987, Tectonic significance of an early Proterozoic two-province boundary in central Arizona: Geol. Soc. America Bull., v. 99, p. 529–538.

Kennedy, G. C., 1950, A portion of the system silica-water: ECON. GEOL., v. 45, p. 629–653.

Kothavala, R. Z., 1963, Wall rock alteration at the United Verde mine, Jerome, Arizona: Unpub. Ph.D. dissert., Harvard Univ., 112 p.

Kranidiotis, P., and MacLean, W. H., 1987, Systematics of chlorite alteration at the Phelps Dodge massive sulfide deposit, Matagami, Quebec: ECON. GEOL., v. 82, p. 1898–1911.

Lanphere, M. A., 1968, Geochronology of the Yavapai series of central Arizona: Canadian Jour. Earth Sci., v. 5, p. 757–762.

Larson, P. B., 1984, Geochemistry of the alteration pipe at the Bruce Cu-Zn volcanogenic massive sulfide deposit, Arizona: ECON. GEOL., v. 79, p. 1880–1896.

LeMaitre, R. W., 1976, The chemical variability of some common igneous rocks: Jour. Petrology, v. 17, p. 589–637.

Lesher, C. M., Lindberg, P. A., and Cambell, I. H., 1986, Trace

element mobility in the Cleopatra crystal tuff, Jerome, Arizona [abs.]: Geol. Soc. America Abstracts with Programs, v. 18, p. 672.

Lindberg, P. A., 1986a, A brief geologic history and field guide to the Jerome district, Arizona, *in* Nations, J. D., Conway, C. M., and Swann, G. A., eds., Geology of central and northern Arizona: Geol. Soc. America, Rocky Mountain Sec. Mtg. Guidebook, p. 127–139.

—— 1986b, An overview of Precambrian ore deposits of southwestern United States: Geol. Soc. Arizona Digest, v. 16, p. 18–23.

—— 1988, Precambrian ore deposits of Arizona, *in* Geology of Arizona: Geol. Soc. Digest Arizona, in press.

Lindberg, P. A., and Gustin, M. S., 1987, Field trip guide to the geology, structure and alteration of the Jerome Arizona ore deposits, *in* Field trip guidebook: Geologic diversity of Arizona and its margins: Geol. Soc. America Ann. Mtg., 100th, p. 176–181.

Lindberg, P. A., and Jacobson, H. S., 1974, Economic geology and field guide to the geology, structure and alteration of the Jerome, Arizona ore deposits, *in* Geology of northern Arizona, II. Area studies and field guides: Geol. Soc. America Rocky Mountain Sec. Mtg., Flagstaff, Arizona, p. 794–804.

MacGeehan, P. J., 1978, The geochemistry of altered volcanic rocks at Matagami, Quebec: A geothermal model for massive sulfide genesis: Canadian Jour. Earth Sci., v. 15, p. 551–570.

Mizukami, M., and Ohmoto, H., 1983, Controlling mechanisms for the major element chemistry of aqueous solutions in tuff-rich environments: ECON. GEOL. MON. 5, p. 559–569.

Morton, R. L., and Nebel, M. L., 1984, Hydrothermal alteration of felsic volcanic rocks at the Helen siderite deposit, Wawa, Ontario: ECON. GEOL., v. 79, p. 1319–1333.

Mottl, M. J., and Holland, H. D., 1978, Chemical exchange during hydrothermal alteration of basalt by seawater—I. Experimental results for major and minor components of seawater: Geochim. et Cosmochim. Acta, v. 42, p. 1103–1115.

Mottl, M. J., Holland, H. D., and Corr, R. F., 1979, Chemical exchange during hydrothermal alteration of basalt by seawater—II. Experimental results for Fe, Mn and sulfur species: Geochim. et Cosmochim. Acta, v. 43, p. 869–884.

Muehlenbachs, K., 1986, Alteration of oceanic crust and the $\delta^{18}O$ history of seawater: Rev. Mineralogy, v. 16, p. 425–443.

Nash, J. T., 1973, Microprobe analyses of sericite, chlorite and epidote from Jerome, Arizona: U. S. Geol. Survey Jour. Research, v. 1, p. 673–678.

Ohmoto, H., 1972, Systematics of sulfur and carbon isotopes in hydrothermal ore deposits: ECON. GEOL., v. 67, p. 551–578.

Ohmoto, H., Mizukami, M., Drummond, S. E., Eldridge, C. S., Pisutha-Arnond, V., and Lenagh, T. C., 1983, Chemical processes of kuroko formation: ECON. GEOL. MON. 5, p. 570–604.

Pisutha-Arnond, V., and Ohmoto, H., 1983, Thermal history, and chemical and isotopic compositions of the ore-forming fluids responsible for the kuroko massive sulfide deposits in the Hokuroku district of Japan: ECON. GEOL. MON. 5, p. 523–558.

Polya, D. A., Solomon, M., Eastoe, C. J., and Walshe, J. L., 1986, The Murchison Gorge, Tasmania—a possible cross section through a Cambrian massive sulfide system: ECON. GEOL., v. 81, p. 1341–1355.

Reber, L. E., Jr., 1938, Jerome district: Arizona Bur. Mines Bull., v. 145, p. 41–65.

Reed, M. H., 1982, Calculation of multicomponent chemical equilibria and reaction processes in systems involving minerals, gases and an aqueous phase: Geochim. et Cosmochim. Acta, v. 46, p. 513–528.

Roberts, R. G., and Reardon, J., 1978, Alteration and ore-forming processes at Mattagami Lake mine, Quebec: Canadian Jour. Earth Sci., v. 15, p. 2–21.

Seyfried, W. E., and Mottl, M. J., 1982, Hydrothermal alteration of basalt by seawater under seawater-dominated conditions: Geochim. et Cosmochim. Acta, v. 46, p. 985–1002.

Sleep, N. H., and Wolery, I. J., 1978, Egress of hot water from midocean ridge hydrothermal systems: Some thermal constraints: Jour. Geophys. Research, v. 83, pt. B12, p. 5913–5922.

Solomon, M., Walshe, J. L., and Eastoe, C. J., 1987, Experiments on convection and their relevance to the genesis of massive sulfide deposits: Australian Jour. Earth Sci., v. 34, p. 311–323.

Spooner, E. T. C., 1977, Hydrodynamic model for the origin of the ophiolitic cupriferous pyrite ore deposits of Cyprus: Geol. Soc. London, Spec. Paper 7, p. 58–71.

Taylor, H. P., 1968, The oxygen isotope geochemistry of igneous rocks: Contr. Mineralogy Petrology, v. 19, p. 1–71.

Turner, F. J., and Verhoogen, J., 1960, Igneous and metamorphic petrology, 2nd ed.: New York, McGraw-Hill Book Co., 694 p.

Urabe, T., Scott, S. D., and Hattori, K., 1983, A comparison of footwall-rock alteration and geothermal systems beneath some Japanese and Canadian volcanogenic massive sulfide deposits: ECON. GEOL. MON. 5, p. 345–364.

Vance, R. K., and Condie, K. C., 1987, Geochemistry of footwall alteration associated with the early Proterozoic United Verde massive sulfide deposit, Jerome, Arizona: ECON. GEOL., v. 82, p. 571–586.

Velde, B., and Medhioub, M., 1988, Approach to chemical equilibrium in diagenetic chlorites: Contr. Mineralogy Petrology, v. 98, p. 122–127.

Walshe, J. L., 1986, A six-component chlorite solid solution model and the conditions of chlorite formation in hydrothermal and geothermal systems: ECON. GEOL., v. 81, p. 681–703.

Walshe, J. L., Hedges, M. M., and Harrold, B. P., 1986, Evaluation of the conditions of chlorite formation in hydrothermal and geothermal systems [abs.]: Water-Rock Interaction Meeting, 5th, Iceland, Abstracts.

Winkler, H. J. F., 1979, Petrogenesis of metamorphic rocks: New York, Springer-Verlag, 348 p.

Zierenberg, R. A., Shanks, W. C., III., Seyfried, W. E., Jr., Koshki, R. A., and Strickler, M. D., 1988, Mineralization, alteration and hydrothermal metamophism of the ophiolite-hosted Turner-Albrite sulfide deposit, SW Oregon: Jour. Geophys. Research, v. 93, pt. B5, p. 4657–4674.